eLife

Reviewed Preprint
v1 • June 4, 2026
Not revised

For correspondence:
mitchellrey.toleco@uis.no
mark.vandergiezen@uis.no

$ Present address: Evolution of Protist Symbioses Laboratory, Institute of Parasitology, Biology Centre, Czech Academy of Sciences, Ceske Budejovice, Czech Republic

Competing interests: No competing interests declared

Funding: See page 25

Reviewing editor: Gertraud Burger, Université de Montréal, Canada

A genetic toolkit for stable episomal transgenesis in the anaerobic gut parasite *Blastocystis* ST7-B

M Rey Toleco[1,$], Kevin SW Tan[2], Mark van der Giezen[1,3,4]

[1]Department of Chemistry, Bioscience, and Environmental Engineering, University of Stavanger, Stavanger, Norway • [2]Laboratory of Molecular and Cellular Parasitology, Healthy Longevity Translational Research Programme and Department of Microbiology and Immunology, Yong Loo Lin School of Medicine, National University of Singapore, Singapore, Singapore • [3]Research Department, Stavanger University Hospital, Stavanger, Norway • [4]Natural Resources Institute, University of Greenwich, London, United Kingdom

eLife Assessment

This paper presents a **valuable** methodology for genetic manipulation of Blastocystis. Although some imaging data are **compelling**, higher-quality figures together with more rigorous biochemical assays would strengthen support for the authors' claims. With the experimental evidence and graphics improved, the study would be of interest both to researchers investigating mitochondrial evolution under anaerobic conditions and to medical biologists studying human pathogens.

https://doi.org/10.7554/eLife.111816.1.sa3

Abstract

Blastocystis is among the most prevalent microbial eukaryote in the human gut, yet it has remained largely inaccessible to functional genetics. Here, we report a combinatorial toolkit for *Blastocystis* ST7-B that enables stable episomal transgene maintenance under antibiotic selection and recovery of colony-derived transgenic lines. Guided by a proteomics-informed candidate screen, we identified endogenous promoter–terminator pairs and benchmark their activity using NanoLuc luciferase (Nluc), defining near-background, weak, intermediate, and robust expression tiers. We optimise square-wave electroporation and establish conditions that balance DNA delivery with culture viability, providing a practical operating regime for routine transfection. Using resazurin-based viability assays alongside culture outgrowth validation, we identified puromycin and trimethoprim as the most reliable selectable systems. A three-stage workflow combining liquid enrichment, solid-phase selection, and liquid culture expansion supports recovery of colony-derived transgenic lines that can be cryopreserved and revived with retained growth, antibiotic resistance, and reporter expression. Finally, bicistronic constructs incorporating a codon-optimised P2A peptide supported selection-linked expression of anaerobic-compatible reporters (UnaG, smURFP, and SNAP-tag). Results showed reporter-dependent performance consistent with constraints such as chromophore availability and substrate permeability. Together, these make *Blastocystis* ST7-B markedly more amenable to genetic engineering.

Introduction

Blastocystis is an anaerobic microbial eukaryote that colonises the intestinal lumen of its host under extremely low oxygen tension (Stensvold and van der Giezen, 2018). Genetically diverse and morphologically variable, it colonises a wide range of hosts, including humans (Tan, 2008). It is also one of the most prevalent eukaryotic microorganisms in the human gut, with a global

colonisation estimate ranging from one to two billion individuals (Scanlan and Stensvold, 2013). Yet mechanistic understanding remains limited, particularly with respect to its metabolic physiology and interaction with its host.

At least 44 distinct subtypes (STs) have been identified based on small subunit ribosomal RNA gene sequences, with ST1 to ST9 found in humans (Koehler et al., 2024; Šejnohová et al., 2024). Among these, ST1-4 are the most frequently detected in human microbiomes (Alfelani et al., 2013). Recently, the presence of *Blastocystis* in the gut was reported to correlate with favourable cardiometabolic profiles and lower BMI values, and negatively associated with diseases linked to altered gut ecology (Piperni et al., 2024). However, such generalisations obscure important subtype-specific differences that shape its biology. In animal models, *Blastocystis* ST7-B has been associated with shifts in microbiome composition that includes reduced abundance of beneficial taxa, whereas *Blastocystis* ST4-WR1 has been linked to the opposite trend (Yason et al., 2019; Deng and Tan, 2022). In epithelial cell culture, several ST7 isolates trigger tight junction disruption, whereas the ST4 isolates tested did not (Wu et al., 2014). These paradoxical subtype-specific effects complicate any attempt to classify *Blastocystis* as strictly commensal or pathogenic (Deng and Tan, 2025).

Blastocystis metabolism is equally unconventional. It encodes both the classical mitochondrial pyruvate dehydrogenase complex and the anaerobic pyruvate:ferredoxin oxidoreductase (PFO), consistent with the potential for dual modes of pyruvate decarboxylation (Stechmann et al., 2008). It encodes an iron-only [FeFe] hydrogenase, typically linked to molecular hydrogen generation, though hydrogen production has not been detected under the conditions tested in *Blastocystis* (Stechmann et al., 2008). Its tricarboxylic acid (TCA) cycle is incomplete, missing key enzymes such as citrate synthase and isocitrate dehydrogenase, and may function in malate dismutation rather than canonical respiration (Stechmann et al., 2008; Gentekaki et al., 2017). Intriguingly, *Blastocystis* expresses alternative oxidase (AOX), a mitochondrial enzyme that uses oxygen as a terminal electron acceptor, although its physiological relevance remains unresolved (Tsaousis et al., 2018). Together, these features reflect the hybrid and evolutionarily distinct nature of its mitochondria.

A further hallmark of *Blastocystis* physiology is mitochondrial glycolysis, where multiple glycolytic enzymes localise to the mitochondria (Abrahamian et al., 2017; Bártulos et al., 2018; Pyrihova et al., 2024). By relocating core carbon flux across the cytosol–mitochondria boundary, this organisation implies rewired redox and ATP economics and makes *Blastocystis* a useful experimental system for testing how metabolism and organelle function co-evolve under anaerobic constraint. A link between mitochondrial glycolysis and serine biosynthesis has been proposed in oomycetes (Abrahamian et al., 2017), but does not apply to *Blastocystis*, which does not encode mitochondrial versions of the key enzymes required for serine biosynthesis. In parallel, comparative genomics supports a trajectory of reductive evolution, including a streamlined genome and coordinated loss of peroxisomes and flagella, consistent with long-term adaptation to an anaerobic gut niche (Gentekaki et al., 2017; Záhonová et al., 2023).

Though *Blastocystis* occupies a unique position at the intersection of metabolic specialisation, reductive evolution, and global gut colonisation, it remains refractory to molecular-level experimental manipulation. Without functional genetics, mechanistic insight across cellular, metabolic, and ecological dimensions remains speculative. A major step toward genetic manipulation in *Blastocystis* ST7-B was achieved with the development of an episomal expression system for transient transfection (Li et al., 2019). This approach employed a species-specific promoter derived from the upstream region of the legumain gene, paired with its native 3' UTR containing a conserved motif downstream of the polyadenylation signal essential for expression (Klimbarš et al., 2014). Among the regulatory elements tested, this was the only combination shown to reliably drive transgene expression. Furthermore, the system was constrained by low transfection efficiency, dependence on a single validated promoter–terminator pair, and the absence of effective drug-selectable markers at the time. These limitations prevented sustained expression, precluded clonal propagation, and restricted functional studies that rely on persistent gene activity. Addressing these gaps will require further optimisation, including identification of

additional endogenous regulatory elements, development of robust selection strategies, and establishment of methods for stable transgene maintenance and clonal line generation. Because transfection has been demonstrated in *Blastocystis* ST7-B, it provides a practical entry point for systematic tool development.

To address these gaps, we developed a genetic toolkit for *Blastocystis* ST7-B. It combines an optimised electroporation workflow for DNA delivery, a screened set of endogenous promoters and terminators for expression control, validated antibiotic markers for selection, and reporter readouts based on P2A-linked constructs and anaerobic-compatible fluorescent proteins.

This combinatorial toolkit establishes *Blastocystis* ST7-B as a genetically accessible system for studying the regulatory logic of its unorthodox cellular physiology and probing organellar evolution under anaerobic constraint. By enabling sustained transgene expression under drug selection, reporter-based assays, and colony-derived transgenic line generation, it provides an entry point for mechanistic experiments on colonisation-relevant traits and subtype-linked host interaction readouts. Beyond its application to *Blastocystis*, the toolkit offers a transferable framework for molecular tool development in other non-model microbial eukaryotes. By prioritising endogenous regulatory elements, modular construct architecture, and empirical optimisation, this work offers an actionable blueprint for bringing molecular genetics to lineages that remain inaccessible to molecular investigation.

Methods

Cell culture

Axenic cultures of *Blastocystis* ST7-B were maintained in pre-reduced Iscove's Modified Dulbecco's Medium (IMDM) with stable glutamine in 25 mM HEPES (L0191; Biowest) supplemented with 10% (v/v) heat-inactivated horse serum (Gibco). Cultures were incubated at 37 °C under anaerobic conditions in 2.5 L anaerobic jars with an anaerobic gas pack (Oxoid) for 3 to 4 days, or until a marked increase in cell density was evident, typically accompanied by a colour change in the medium.

Promoter and terminator selection

Candidate sources of promoter and terminator sequences were genes identified from a published proteomic dataset of *Blastocystis* ST4-WR1 (Armengaud et al., 2017) whose transcripts were annotated with a conserved motif downstream of polyadenylation signal within the 3' untranslated region (3' UTR). Selection focused on the 1,000 most abundant proteins to establish a preliminary library of putative cis-regulatory elements capable of supporting varying levels of transcriptional activity. Orthologs in the *Blastocystis* ST7-B genome were identified via BLAST searches (Altschul et al., 1990; Camacho et al., 2009) and retained if they exhibited ≥60% query coverage and ≥75% percent identity. These filters were chosen to reduce spurious matches while preserving clear homologs. For each retained orthologous gene, the putative promoter region was defined as the intergenic sequence upstream of the start codon, extending to the predicted 3' UTR boundary of the adjacent gene on the same DNA strand; in some loci, these regions extended into the neighbouring gene's coding sequence. Alternative promoter lengths were considered based on available intergenic space and evaluated individually according to locus-specific constraints. Candidate terminator regions were defined as the 500 bp immediately downstream of the stop codon.

Cloning

All cloning was performed using the in-house protocol (Toleco and van der Giezen, 2025) adapted from the NEBuilder HiFi DNA Assembly kit (NEB). Plasmids were sent to Microsynth AG (Germany) for Sanger sequencing. For large-scale plasmid preparation, maxi- or giga-preps were carried out using commercial kits (Qiagen) or the Miraprep method (Pronobis et al., 2016). Selection marker genes (*Ecdhfr*, *Hsdhfr*, and *pac*) and anaerobic fluorescent reporter genes (*UnaG*, *smURFP*, and *SNAP-tag*®) were codon-optimized for *Blastocystis* ST7-B and synthesized by

Invitrogen GeneArt Gene Synthesis Services (Thermo Fisher Scientific; Supplemental Data 1). All oligonucleotides were designed using Benchling (*https://benchling.com*) and ordered from Thermo Fisher Scientific (Supplemental Table 1).

Estimation of IC_{50}

Estimation of IC_{50} using rezasurin was done as described by Mirza et al. (2011). Antibiotics tested were puromycin (Thermo Fisher Scientific), trimethoprim (MedChemExpress), and WR99210 (MedChemExpress); an additional lot of WR99210 was provided by Jacobus Pharmaceutical (NJ, USA) as a generous gift.

Transfection protocol

The basic transfection protocol was adapted from Li et al. (2018) with modifications. *Blastocystis* ST7-B cells, cultured for 2–3 days, were harvested by centrifugation at 1,000 x g for 5 minutes at room temperature. The pellet was washed with 5 mL of pre-reduced, incomplete cytomix buffer (10 mM K_2HPO_4/KH_2PO_4, pH 7.6, 120 mM KCl, 0.15 mM $CaCl_2$, 25 mM HEPES, 2 mM EGTA, and 5 mM $MgCl_2$) and gently vortexed. Cells were pelleted again under the same conditions, and the supernatant was removed by decanting or gentle vacuum suction, leaving approximately 0.5 mL of buffer above the cell pellet. One millilitre of complete cytomix buffer (pre-reduced incomplete cytomix buffer supplemented with 2 mM ATP and 5 mM glutathione, prepared immediately before use) was added, and the pellet was gently resuspended. Total viable cells were counted using a hemacytometer.

Each transfection was carried out using 5 x 10^7 cells and 25 µg of plasmid DNA. The total electroporation volume was adjusted to 500 µL with complete cytomix buffer. After electroporation, the contents were transferred into a 2 mL microcentrifuge tube using a sterile 1.5 mL Pasteur pipette. The electroporation cuvette was rinsed with 1 mL of complete IMDM medium, and the rinse was pooled with the transfected cells. Cells were centrifuged at 1,000 x g for 5 minutes at room temperature. The supernatant was discarded, and 1.8 mL of complete IMDM was added. The pellet was resuspended by gentle pipetting or flicking of the tube. Further electroporation details are described in the main text. Cultures were incubated under standard conditions inside an anaerobic box (Oxoid) with an anaerobic gas pack (Oxoid), as described above.

Nluc assay

Cells were harvested 16–18 hours post-transfection by centrifugation at 10,000 x g for 2 minutes at 4 °C. The supernatant was discarded, and the pellet was washed with 500 µL sterile PBS. After a second centrifugation under the same conditions, the pellet was resuspended in 350 µL PBS, and 200–300 mg of sterile zirconia beads (Ø 0.1 mm; Biospec) were added. Tubes were placed on ice, and the TissueLyser LT (Qiagen) adapter was flash-frozen in liquid nitrogen for no longer than 2 seconds. Lysis was carried out using the TissueLyser LT at 50 Hz for two cycles of 2 minutes each, with cooling on ice between cycles. The lysate was clarified by centrifugation at 17,000 x g for 10 minutes at 4 °C, and the supernatant was transferred to a fresh 1.5 mL microcentrifuge tube to serve as crude lysate for luciferase assays. For each reaction, 100 µL of crude lysate was mixed with 50 µL Nano-Glo® Luciferase Assay Reagent (Promega) in a luminescence-compatible 96-well plate, protected from direct light, and incubated at room temperature for 10 minutes. Luminescence was measured using SpectraMax iD5 plate reader (Molecular Devices) following 30 seconds of orbital shaking. All assays were performed in three independent electroporation runs and analysed in technical duplicates; mock-transfected (no plasmid DNA) cells were included as negative control.

Selection strategy and clonal propagation

The selection strategy was carried out in phases: liquid phase and solid phase selections followed by re-establishment of the liquid culture. In the liquid phase selection, transfected cells were allowed to recover and propagate until the medium turned yellow without drug treatment. Cells

were then pelleted by centrifugation at 1,500 x g for 5 minutes at room temperature. The supernatant was discarded, and the pellet was resuspended in fresh, pre-reduced IMDM supplemented with antibiotic. The antibiotic concentrations and the graded selection strategy are described in detail the main text.

Once cells had adapted to high dose antibiotic concentrations, they were subjected to solid-phase selection. Cultures were diluted with pre-reduced PBS or IMDM to a final density of 1,000 cells/mL. A 200 to 300 µL aliquot of the diluted cell suspension was spread onto pre-reduced IMDM plates containing 1% agar and 0.1% sodium thioglycolate using a sterile cell spreader (Tan et al., 1996a; Tan et al., 1996b; Tan et al., 2000). Plates were incubated overnight, agar-side down, to allow cells to settle. The following day, plates were inverted and incubated for 10–14 days until visible colonies appeared. Individual colonies were picked and transferred to 2 mL microcentrifuge tubes (with perforated lids for gas exchange), containing 1.8 mL of fresh, pre-reduced IMDM and cultured until the medium turned yellow. These clonal lines were subjected to the same liquid phase selection regime and ultimately maintained at a high drug dose referred to as maintenance concentration.

All incubations were carried out at 37 °C under anaerobic conditions as described above. For contamination control, media were supplemented with an antibiotic cocktail (ABC) comprised of penicillin G (100 U/mL), streptomycin (100 µg/mL), levofloxacin (25 µg/mL), and polymyxin B (100 U/mL).

Confocal Laser Scanning Microscopy

Sample preparation for confocal laser scanning microscopy (CLSM) was adapted from Pyrihová et al. (2024), with minor modifications. All imaging were carried out on circular No. 1.5 glass coverslips (Marienfeld) pre-coated with poly-D-lysine (Gibco).

For UnaG visualisation, washed transgenic *Blastocystis* ST7-B cells were treated with 50 µM bilirubin (BR; Thermo Fisher Scientific), and incubated anaerobically at 37°C for 1 h. Cells were washed twice with PBS before mounting. Wild-type (WT) cells processed in parallel served as controls.

For smURFP imaging, prepared transgenic cells were permeabilized with 0.1% saponin (Thermo Fisher Scientific) for 10 min and washed twice with pre-reduced PBS. Permeabilized cells were then incubated with 50 µM biliverdin (BV; Merck) under anaerobic conditions at 37 °C for 2 h, washed twice with PBS, and mounted for imaging. WT cells treated identically were used as controls.

For SNAP-tag® imaging, cells were incubated with SNAP-Cell® TMR-Star (NEB) at 0, 3, and 5 µM concentrations for 30 min at 37 °C under anaerobic conditions. Cells were washed twice with PBS prior to mounting. As controls, the same SNAP-tag®–expressing *Blastocystis* ST7-B line incubated without substrate was used as control experiment.

All imaging protocols used the same wash regime to remove excess substrate, and cells were counterstained with Hoechst 33342 (Molecular Probes) to visualize DNA. Cells were mounted in ProLong Gold Antifade Mountant (Molecular Probes), sealed with colourless nail polish, and cured overnight prior to image acquisition.

Confocal image stacks were acquired on a Leica TCS SP8 laser-scanning confocal microscope equipped with a 63x/1.40 NA oil-immersion objective (Leica Microsystems). Z-stacks were collected using system-optimized sampling compliant with the Nyquist–Shannon sampling theorem and LAS X LIGHTNING deconvolution-optimized settings (Leica Microsystems), except during SNAP-tag® imaging due to technical issues with our microscope. Laser power, pinhole diameter and other imaging settings were kept constant within each fluorescent reporter system to allow unbiased visual comparison of fluorescence intensities across conditions. For presentation, a subset of optical sections (10 consecutive slices) was collapsed into a maximum-intensity Z-projection. The linear dynamic range for each signal channels was kept constant across treatments.

Single transmitted-light slices were background-corrected using the rolling-ball algorithm (radius 60 px; light background; sliding paraboloid and smoothing enabled) to better visualize cellular morphology relative to the fluorescence signals. The background-corrected transmitted-light images were then overlaid with the corresponding fluorescence channels in the final merged images, and a cell outline was manually traced to approximate cellular boundaries. All image processing was performed in Fiji (ImageJ distribution, version 1.54p).

Statistical analysis

Data distributions and variance patterns were examined, and the assumptions for parametric testing were not met. Consequently, group differences were evaluated with the Kruskal–Wallis rank-sum test. When omnibus results were significant, post-hoc pairwise comparisons were performed using Dunn's test with P-values adjusted for multiple comparisons using Benjamini–Hochberg method. Unless noted otherwise, tests were two-sided with $\alpha = 0.05$. Dose–response curves were estimated via nonlinear regression of sigmoidal dose–response models. Analyses were conducted in R (version 4.5.1) and GraphPad Prism (10.6.1 (892))

Results

Endogenous promoter–terminator pairs support graded transgene expression in *Blastocystis* ST7- B

Transgene expression in *Blastocystis* ST7-B has so far relied on a single validated endogenous promoter–terminator pair from the legumain locus (LeguP1; Li et al., 2018). To expand the set of regulatory parts available for construct design, we benchmarked 23 endogenous promoter–terminator combinations from 14 candidate loci using an Nluc reporter in *Blastocystis* ST7-B (Table 1; Figure1A). Reporter output across three independent transfections per construct spanned a broad range, from near-background to values approaching the LeguP1 reference, with some individual replicates exceeding the reference measured in parallel. Robust signals were obtained with SARFGBPpro-600, 60SRPL3pro-1000, and EamApro-1023, while 60SRPL3pro-500, EamApro-1245, AATpro-1000, and SARFGBPpro-1325 showed moderate activity (Figure 2A). These constructs therefore expand the set of endogenous regulatory elements that support detectable to strong transgene expression in *Blastocystis* ST7-B.

Most of the remaining constructs produced weak reporter output relative to LeguP1, and several remained negligible or near-background, including AALpro-1000, AALpro-1500, CBMCPpro-378, and CBMCPpro-572. For AAL and CBMCP, increasing promoter length did not improve activity under the conditions tested. Candidate selection had been guided by *Blastocystis* ST4-WR1 protein abundance and the presence of a conserved GU-rich 3' UTR motif, but these features did not reliably predict regulatory performance in *Blastocystis* ST7-B. For example, although AAL is associated with high protein abundance in *Blastocystis* ST4-WR1 and contains the GU-rich 3' UTR motif, both AAL promoter fragments drove only near-background expression in *Blastocystis* ST7-B (Figure 2A).

P2A supports selection-linked co-expression in *Blastocystis* ST7-B

To add a bicistronic expression option in *Blastocystis* ST7-B, we inserted a codon-optimised P2A sequence into a LeguP1-driven cassette linking a selectable marker and UnaG reporter (Figure 1B). UnaG was used because GFP-family fluorophores require oxygen for chromophore maturation and are therefore unsuitable for anaerobic systems. Before drug selection, fluorescence microscopy of bulk-transfected cultures detected a subset of UnaG-positive cells, indicating expression from the bicistronic construct (Figure 3A). After puromycin selection, UnaG-positive cells were retained and enriched in the surviving population. These results are consistent with functional P2A-linked co-expression of both a selectable marker and a reporter protein in *Blastocystis* ST7-B.

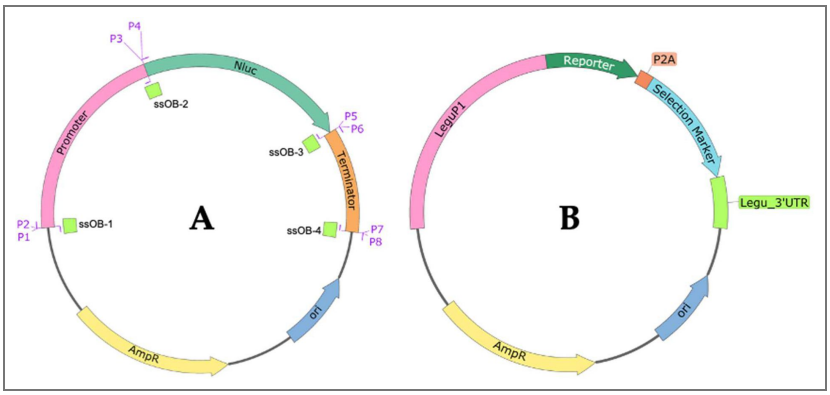

Figure 1.

(**A**) Schematic of the plasmid architecture used to assay promoters and terminators using Nluc as reporter. Coloured blocks/arrows denote interchangeable modules; P1-P8 (purple) represent the necessary primers to PCR amplify the DNA fragments for assembly and green fragments represent the ssOBs needed to complete the DNA assembly reaction. This configuration highlights the modularity of the approach. Plasmids were cloned and amplified in *E. coli* and then introduced into *Blastocystis* ST7-B, functioning in practice as an *E. coli* ↔ *Blastocystis* ST7-B shuttle vector. Robust expression and drug selection were obtained without adding a *Blastocystis*-specific or canonical eukaryotic origin of replication (e.g., 2μ in yeasts or SV40 ori in mammalian cells), indicating that sequences in the bacterial backbone were sufficient for plasmid maintenance in *Blastocystis* ST7-B. (**B**) A bicistronic construct model using P2A peptide to enable co-expression of a fluorescent reporter and a selectable marker under a single promoter-terminator pair. Reporters used were UnaG, smURFP, and SNAP-tag®; selection markers were *Ecdhfr* (trimethoprim) and *pac* (puromycin).

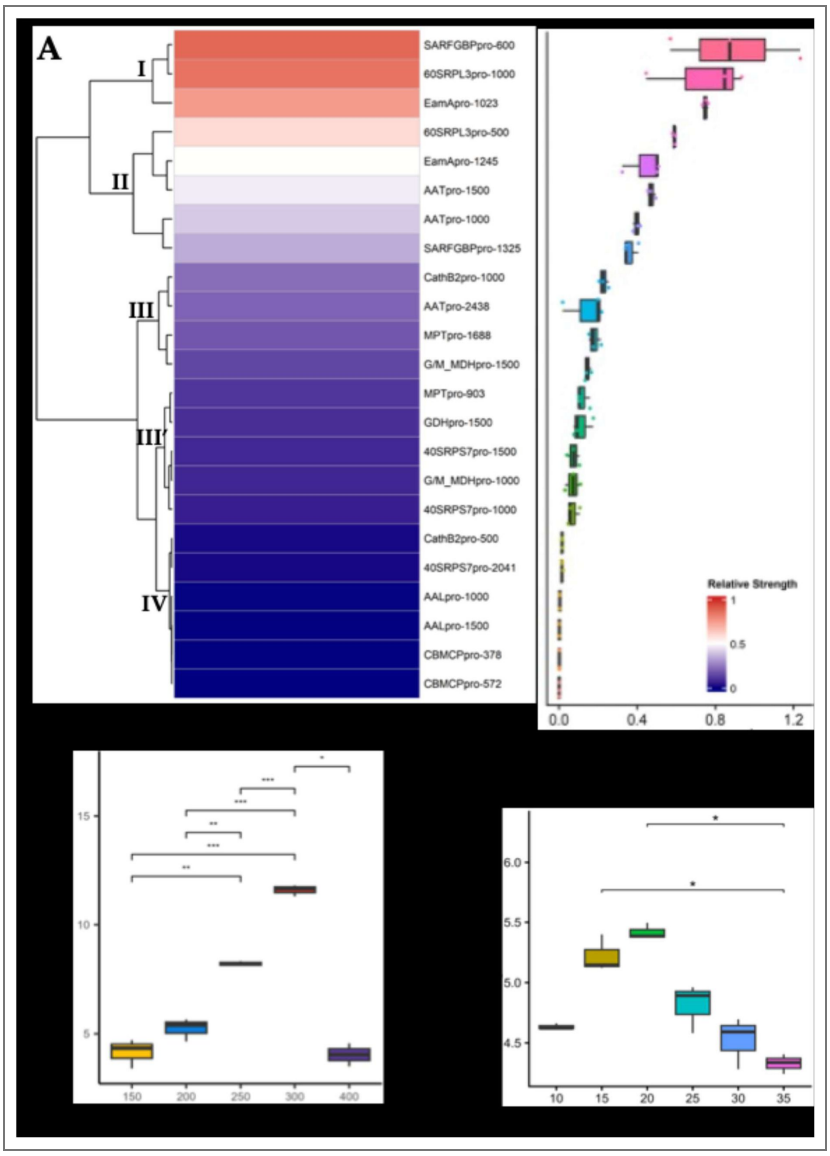

Figure 2.

(**A**) Heatmap with hierarchical clustering (left) and boxplots (right) of promoter–terminator activity in *Blastocystis* ST7-B. Activity was measured by Nluc luminescence. For each construct, raw relative light units (RLU; n = 3 independent replicates) were normalized to the LeguP1 reference construct (external standard) to obtain relative strength. Values are displayed on a 0–1 scale using min–max scaling after normalization; on this scale, 1.0 corresponds to the LeguP1 reference. Promoter fragment lengths are indicated by the numbers in the labels. Unsupervised clustering resolved, into tiers: (I) robust, (II) moderate, (III and III') weak, and (IV) negligible. In the adjacent boxplots, points represent individual replicate values. (**B**) Effect of square-wave voltage on Nluc luminescence (RLU; n = 3 independent replicates per condition) with pulse duration fixed at 30 ms. (**C**) Effect of single pulse duration on luminescence signal (RLU; n = 3 independent replicates per condition) voltage fixed at 300 V. For **B** and **C**, electroporation runs were performed with a single pulse while plasmid amount and cell density were held constant. Boxplots show log-transformed raw RLU values (not normalized). Group differences were assessed by Kruskal–Wallis followed by Dunn's post hoc test (α = 0.05); brackets mark tested contrasts and *, **, *** indicate $P < 0.05$, 0.01, 0.001, respectively. Although the 20 ms pulse was not significantly different from 15, 25, or 30 ms, it was chosen for subsequent electroporation runs because it produced the narrowest interquartile range (least dispersion) while maintaining a high signal.

Table 1. Genes from which endogenous promoters and terminators were cloned to drive transgene expression in *Blastocystis* ST7-B.

Blastocystis ST4-WR1			*Blastocystis* ST7-B				
Abundance Ranking*	**NCBI protein accession No.**	**Protein Name†**	**ST7-B Gene Homolog**	**NCBI RefSeq**	**% query coverage**	**% Identity**	**Promoter Lengths Tested‡**
6	XP_014525968.1	aspartate ammonia-lyase; AAL	GSBLH_T000 03689001	NW_01317 1849.1	96.00	89.67	AALpro-1000; AALpro-1500
8	XP_014525496.1	small ADP ribosylation factor GTP-binding protein; SARFGBP	GSBLH_T000 04960001	NW_01317 1868.1	100.00	85.39	SARFGBPpro-600; SARFGBPpro-1325
9	XP_014529056.1	2-amino-3-ketobutyrate coenzyme a ligase; AKBCoAL	GSBLH_T000 00411001	NW_01317 1815.1	69.00	82.98	Cloning Unsuccessful
15	XP_014525225.1	60S ribosomal protein L3; 60SRPL3	GSBLH_T000 04213001	NW_01317 1865.1	100.00	83.22	60SPRPL3pro-500; 60SPRPL3pro-1000
21	XP_014529132.1	aspartate aminotransferase; AAT	GSBLH_T000 01883001	NW_01317 1821.1	89.00	85.14	AATpro-1000; AATpro-1500; AATpro-2438
32	XP_014527004.1	glycine dehydrogenase; GDH	GSBLH_T000 02695001	NW_01317 1827.1	90.00	76.32	GDHpro-1500
87	XP_014525499.1	glyoxysomal and mitochondrial malate dehydrogenases; G/M_MDH	GSBLH_T000 04946001	NW_01317 1868.1	96.00	82.59	G/M_MDHpro-1000; G/M_MDHpro-1500
124	XP_014529593.1	calcium binding mitochondrial carrier protein; CBMCP	GSBLH_T000 03387001	NW_01317 1838.1	100.00	81.97	CBMCPpro-378; CBMCPpro-572
129	XP_014528036.1	40S ribosomal protein S7; 40SRPS7	GSBLH_T000 05110001	NW_01317 1868.1	81.00	79.93	40SRPS7pro-1000; 40SRPS7pro-1500; 40SRPS7pro-2041
348	XP_014526323.1	mitochondrial phosphate transporter; MPT	GSBLH_T000 02675001	NW_01456 9325.1	100.00	80.42	MPTpro-903; MPTpro-1688
535	XP_014529047.1	cathepsin B1; CathB1	GSBLH_T000 05101001	XP_0128995 54.1	96	80.32	Cloning Unsuccessful
		cathepsin B2; CathB2	GSBLH_T000 05101001	XP_0128995 55.1	90	79.84	CathB2pro-500; CathB2pro-1000
595	XP_014525961.1	EamA-like transporter family; EamA	GSBLH_T000 04551001	NW_01317 1866.1	97	75.51	EamApro-1023; EamApro-1245
1000	XP_014526708.1	peptidase C1A family protein; PC1AFP	GSBLH_T000 01253001	NW_01317 1817.1	67	77.31	Cloning Unsuccessful

*Based on the *Blastocystis* ST4-WR1 proteome dataset (Armengaud et al., 2017).

†Protein names are from existing annotations in ST4-WR1 or ST7-B; given abbreviations are arbitrarily assigned for nomenclature convenience.

‡Promoter naming is based on the protein abbreviations used in this work followed by the number of based upstream the start codon. For example, AALpro-1000 means a genomic sequence of 1000 bp upstream of the start codon of aspartate ammonia-lyase (AAL) in *Blastocystis* ST7-B. Unsuccessful cloning means after a second failed cloning attempt.

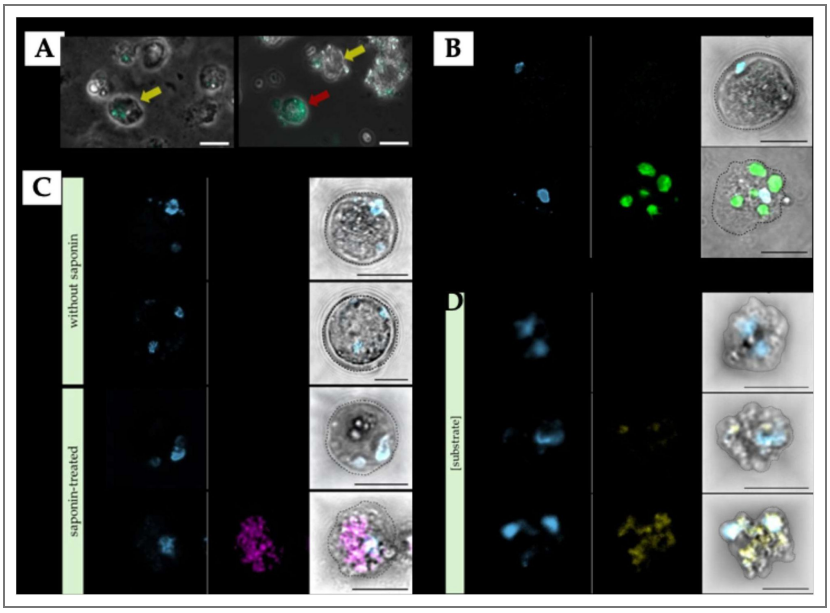

Figure 3.

(A) Fluorescence micrographs of *Blastocystis* ST7-B transfected with LeguP1:UnaG::P2A::pac:LeguTer and imaged 3 days post-transfection before antibiotic selection using an Olympus IX81 fluorescence microscope. Images show phase-contrast overlaid with the UnaG channel. In the absence of exogenous BR, only weak signal is detected, consistent with reported intrinsic autofluorescence in *Blastocystis* (yellow arrows; Nagel et al., 2015). After incubation with 1 mM BR, UnaG-positive cells show strong fluorescence (red arrow), whereas neighbouring non-transformed cells remain at background. Scale bar, 10 µm. (B) Representative single-cell confocal images showing compartmentalised UnaG fluorescence in *Blastocystis* ST7-B after incubation with 50 µM unconjugated BR. WT and UnaG-expressing cells were imaged under identical acquisition settings. For display purposes, the lower threshold of the UnaG channel in the transgenic clone was set to the maximum intensity observed in the WT control, so that only signal above the WT autofluorescence range is visible. (C) smURFP fluorescence in *Blastocystis* ST7-B is limited by chromophore access and is unmasked by saponin permeabilisation. Live cells expressing cytosolic smURFP were incubated with 50 µM BV and imaged by confocal microscopy either without permeabilisation or after treatment with 0.1% saponin. No signal was detected above background without saponin. After permeabilisation, smURFP fluorescence became strong and broadly distributed throughout the cytoplasmic compartment, consistent with the untargeted construct design. (D) SNAP-tag® labelling in *Blastocystis* ST7-B is dependent on substrate availability and concentration and yields broadly distributed fluorescence. Live clones expressing an untargeted cytosolic SNAP-tag® were incubated with increasing concentrations of a cell-permeant benzylguanine fluorophore substrate and imaged by confocal microscopy. Signal was at or near background at low substrate but increased progressively with substrate concentration and became broadly distributed throughout the cytoplasmic compartment, consistent with efficient covalent labelling in live cells. Scale bars in B, C, and D represent 5 µm.

Square-wave electroporation improves DNA delivery culture recovery in *Blastocystis* ST7- B

Applying the time-constant electroporation protocol of Li et al. (2017) at the recommended 370 V frequently caused arcing and loss of viability in *Blastocystis* ST7-B. Under these conditions, cells darkened, settled at the bottom of the tube, failed to recover, and cultures showed no colour change after 3 to 5 days of incubation. Lowering the voltage to 350 V eliminated arcing, but transfection outcomes remained inconsistent across replicates, indicating that reducing voltage alone did not resolve the limited reproducibility. We therefore replaced time-constant operation, which produces exponential voltage decay, with square-wave electroporation, which maintains constant voltage, and optimised the settings empirically using the LeguP1-Nluc reporter construct.

Voltage was first tested across 150 to 400 V using a single 20 ms pulse in 4 mm cuvettes, while cell input, DNA amount, and transfection volume were held constant at 5 x 10^7 cells, 25 µg DNA, and 500 µL, respectively (Figure 2B). At 150 to 200 V, corresponding to 0.375 to 0.50 kV/cm, Nluc signals were low. Reporter output increased sharply at 250 V and peaked at 300 V, corresponding to 0.625 and 0.75 kV/cm, respectively, whereas signal dropped markedly at 400 V even in replicates without visible arcing. Both 250 and 300 V produced strong reporter output without arcing or obvious loss of viability, and cultures showed a colour change within 24 hours, with 300 V giving the strongest performance under matched conditions.

Pulse duration was then tested at fixed voltage by comparing single pulses from 10 to 35 ms at 300 V while holding all other parameters constant (Figure 2C). Reporter output increased from 10 to 20 ms and declined at longer pulse durations, with 20 ms consistently outperforming both shorter and longer pulses across replicates.

Because cuvette geometry, electroporation buffer, DNA amount, cell number, and reaction volume were unchanged across these experiments, the observed differences in reporter output and recovery were most consistent with effects of waveform, voltage, and pulse duration. Square-wave electroporation at 300 V for 20 ms in 4 mm cuvettes was therefore used for subsequent transfections.

Drug sensitivity profiling identifies candidate selection agents for *Blastocystis* ST7-B

To link transgene carriage to cell survival and enable recovery of stable *Blastocystis* ST7-B transformants, we evaluated candidate drugs to establish practical drug–marker pairs for post-transfection selection. Puromycin, trimethoprim, and WR99210 were prioritised because each has a well-established resistance cassette suitable for vector-based expression, namely *pac*, *E. coli* dhfr (*Ecdhfr*), and human DHFR (*Hsdhfr*), respectively (Vara et al., 1985; Asselbergs and Widmer, 1995; Fidock and Wellems, 1997; Remcho et al., 2020). WR99210 was additionally included because a putative DHFR–thymidylate synthase homolog is encoded in the *Blastocystis* ST7-B genome, providing a rationale to test whether this compound inhibits ST7-B growth.

Dose–response assays were performed using a resazurin-based viability readout to quantify drug sensitivity and define working concentration ranges (Figure 4). Cells were exposed to concentrations ranging from 0 to 1.5 µM for each compound, yielding IC_{50} values of 30 ± 6.5 nM for puromycin, 102 ± 24 nM for trimethoprim, and 27 ± 13 nM for WR99210. These values confirm that each compound reduces *Blastocystis* ST7-B viability under the conditions tested. These inhibitory profiles identified puromycin, trimethoprim, and WR99210 as candidate selection agents for further testing, with subsequent experiments supporting puromycin and trimethoprim as the most reliable systems under the conditions used here.

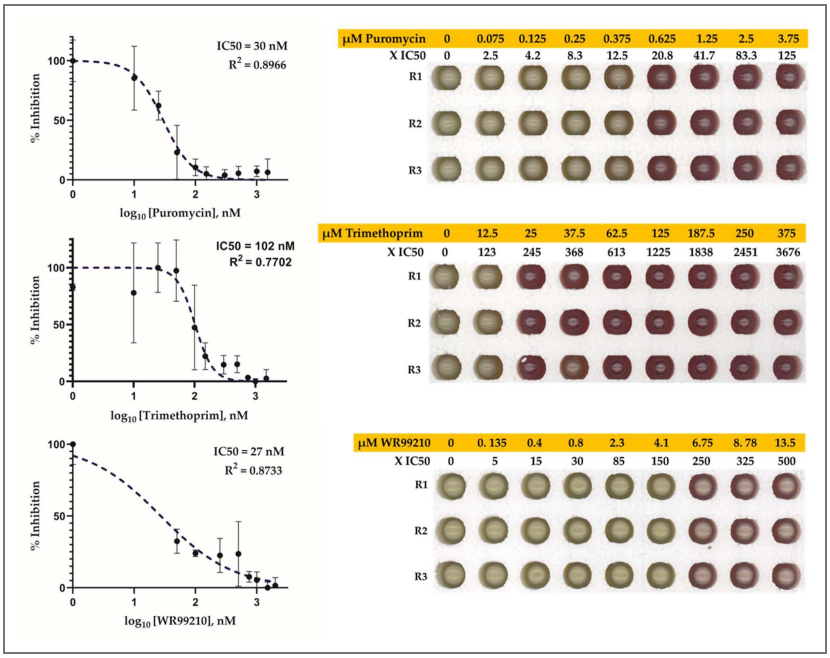

Figure 4. Antibiotic potency and selection-window determination in *Blastocystis* ST7-B.

Dose–response curves for puromycin, trimethoprim, and WR99210 were estimated from a resazurin-based viability assay (n = 3 independent replicates per drug per concentration); points show mean ± SD, and the insets list the estimated IC_{50} values with R^2-values > 0.75 for all fits. Right panels: small culture validation using 1 x 10^7 WT *Blastocystis* ST7-B cells per culture, assayed in triplicates across a wide range of concentrations. Cultures were incubated for 3 days, and viability was assessed by the phenol red pH indicator shift resulting from acidification of the medium, with yellow indicating growth and red indicating no growth. The concentration at the yellow-to-red transition formed the rational basis to develop a selection strategy for *Blastocystis* ST7-B transformants.

Recovery of colony-derived transgenic *Blastocystis* ST7-B lines through by a staged selection regime

To recover *Blastocystis* ST7-B transformants after episomal transfection, we developed a three-stage workflow comprising stepwise antibiotic selection in liquid culture, isolation of single colonies on solid medium, and re-establishment of individual colonies in liquid culture for expansion and verification. Complete growth inhibition (CGI) was defined as the lowest concentration at which no detectable growth occurred over 24 to 48 h. Growth and viability were monitored using simple culture phenotypes: healthy cultures shifted the medium towards yellow and formed dense pellets that resisted resuspension after addition of fresh medium, whereas non-viable cultures retained reddish pink medium and produced pellets that dispersed readily. In 1 x 10^7 WT cells, CGI occurred at 20.8x, 245x, and 250x the provisional IC_{50} for puromycin, trimethoprim, and WR99210, respectively (Figure 4). Direct transfer of transfected populations into CGI-level drug concentrations led to loss of viability, so selection pressure was increased gradually over several passages. Post-electroporation recovery and selection were performed in 2 mL round-bottom microcentrifuge tubes to conserve space and maintain high cell density. To support anaerobiosis while limiting contamination, each snap-cap lid was perforated with a single pinhole, and drug concentration was increased stepwise by pelleting cells, removing supernatant, and resuspending in fresh medium at the next concentration (Figure 5). Because axenisation is difficult in *Blastocystis* (Chen et al., 1997), recovery media were supplemented with penicillin, streptomycin, levofloxacin, and polymyxin B, which suppressed bacterial contaminants without obvious effects on *Blastocystis* ST7-B growth or morphology during routine monitoring.

The solid-phase step yielded colony-derived lines consistent with outgrowth from individual viable units, although not all colonies resumed growth after transfer back into liquid culture, indicating strong density dependence during outgrowth. Recovery improved when plates were inoculated at low density, approximately 200 cells per plate, and incubated for up to 14 days before colony picking. Verification at this stage relied on phenotype and sustained growth under the specified sub-CGI drug concentration, as no growth was observed on plates supplemented at CGI levels, and mock-transformed controls plated in parallel also showed no growth. Across passages, puromycin and trimethoprim consistently discriminated transformed from non-transformed populations. By contrast, WR99210 showed marked source-dependent variability: an initial lot supported inhibition and selection at the expected levels, whereas an independently sourced lot, including freshly prepared stocks, failed to inhibit growth even at concentrations up to 1500× the earlier IC_{50} estimate, and low-passage WT controls no longer reproduced the previous response pattern. ^1H and ^{13}C NMR spectra provided no evidence of WR99210 degradation (data not shown). WR99210 was therefore deprioritised, and puromycin and trimethoprim were used for routine selection in *Blastocystis* ST7-B under these conditions. To reduce repeated sampling of the same lineage during recovery and expansion, three to five electroporation runs were performed per construct, and at least one robust clone from each run was advanced. This workflow enabled recovery of colony-derived transformants that retained drug-resistant growth during extended passaging (>15) and after one year of cryogenic storage.

Anaerobic-compatible fluorescent proteins function in transgenic *Blastocystis* ST7-B lines

To functionally assess transgene expression in *Blastocystis* ST7-B and evaluate the suitability of anaerobic-compatible fluorescent reporters in this organism, three reporters, UnaG, smURFP, and SNAP-tag®, were expressed from bicistronic P2A vectors and examined by confocal microscopy (Kumagai et al., 2013; Rodriguez et al., 2016; Keppler et al., 2003). For each of these proteins, the addition of an external substrate is necessary to form the fluorescent holoenzyme. UnaG, smURFP, and SNAP-tag® requires BR, BV, and SNAP-tag® substrates, respectively. Ultimately, each reporter places different demands on chromophore chemistry and substrate permeability. The

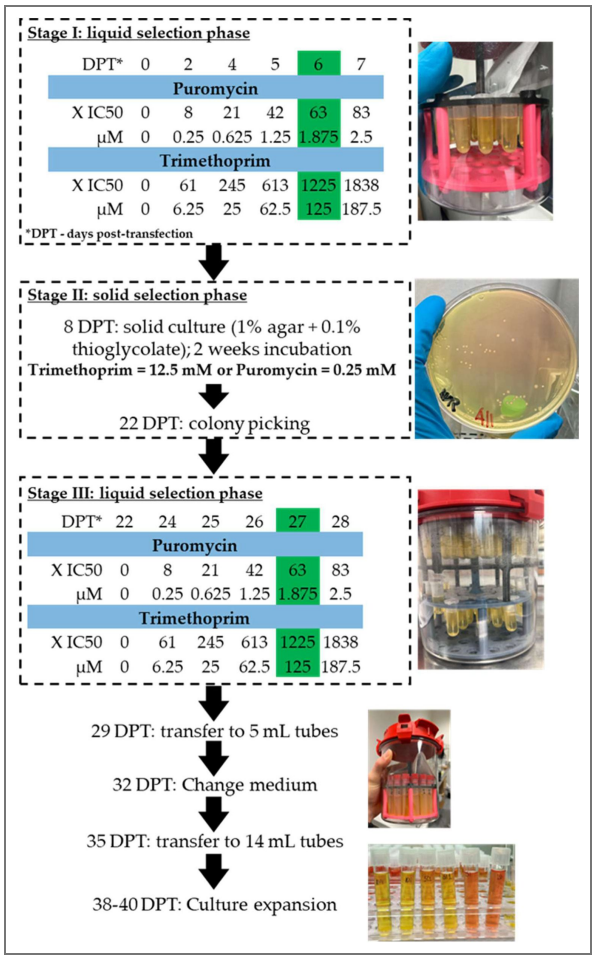

Figure 5. Stepwise selection and clonal propagation of *Blastocystis* ST7-B transformants with puromycin and trimethoprim monitored over days post-transfection (DPT).

Stage I: transfected cells are kept in 2 mL tubes inside anaerobic jars and exposed to increasing drug concentrations; values highlighted in green refer to the maintenance concentration. **Stage II**: enriched cultures are plated on solid medium incubated for 2 weeks, yielding well-isolated colonies that are picked at 22 DPT. At this stage, the drug concentrations are lowered to ensure that individual plated cells, which later form colonies, remain within their resistance capacity during early outgrowth on the plate. **Stage III**: colonies are re-established in liquid culture under the same stepwise antibiotic regime. Subsequently, volume expansion from 2 mL microcentrifuge tubes to 14 mL culture tubes proceeds through an intermediate 5 mL step to increase the success of culture establishment. The entire workflow takes up to 40 days.

P2A constructs combined codon-optimized reporters with selectable markers for puromycin or trimethoprim, and stable episomal resistant lines were isolated and expanded for functional characterization of transgene expression.

UnaG produced a bright green signal that rose clearly above WT autofluorescence when background was subtracted under identical settings. Under these conditions, the UnaG signal was readily detectable and visually robust. Efficient holoenzyme formation was observed without permeabilization of the cells, which indicates that the reporter can become fluorescent *in vivo* (Figure 3B). The UnaG-derived fluorescence did not appear as a uniform cytosolic signal. Instead, it resolved into discrete, bright subcellular foci and larger compartment-like regions, with darker intervening areas that showed little or no fluorescence. The *UnaG* coding sequence used in these constructs lacked any intentional targeting peptide or signal sequence, so the underlying plasmid design was expected to drive broadly ectopic expression throughout the cell.

smURFP expression produced a clean far-red signal in *Blastocystis* ST7-B, but only when cells were permeabilized with 0.1% saponin prior to BV treatment (Figure 3C). Under identical laser power and detector settings, non-permeabilized smURFP-expressing cells remained at background levels that were indistinguishable from WT controls. After saponin treatment, smURFP fluorescence rose clearly above autofluorescence and was readily detectable, confirming that the reporter is expressed and can form a functional holoenzyme in *Blastocystis* ST7-B once the chromophore gains access to the cytoplasm. The smURFP signal appeared specific and free of obvious bleed-through into other imaging channels. Within permeabilized cells, the far-red signal was relatively global across the cytoplasm, without strong restriction to discrete subcellular compartments, consistent with the expected distribution of a broadly expressed cytosolic reporter. This pattern matches the construct design, which did not include any intentional targeting peptide or signal sequence and was therefore anticipated to drive ectopic, global expression.

SNAP-tag® labeling was compatible with *Blastocystis* ST7-B and produced robust fluorescence. In cells expressing SNAP-tag®, addition of a cell-permeant SNAP substrate yielded a clear fluorescent signal across a range of substrate concentrations (Figure 3D).

Signal intensity scaled with substrate dose over the tested range, indicating that labelling efficiency is substrate-limited under standard conditions. Fluorescence appeared broadly distributed throughout the cytoplasm rather than restricted to discrete organelles, which agrees with the construct design that lacks any explicit targeting sequence and is expected to drive ectopic, global expression. Efficient labeling was obtained without semi-permeabilization indicating that the substrate permeated the cell.

Discussion

This study establishes an integrated genetic toolkit for *Blastocystis* ST7-B that links construct design, DNA delivery, antibiotic selection, clonal recovery, and reporter validation into a single experimental pipeline. Its main advance lies not only in any one component alone, but in showing that these elements function together to enable stable episomal transgenesis and downstream cell biological analysis in this organism. The toolkit was intentionally designed as a combinatorial system of interchangeable genetic parts, allowing constructs to be tailored to the desired circuitry through promoter choice, P2A-based bicistronic design, and alternative selection markers or reporters. The previously reported ssOB cloning approach (Toleco and van der Giezen, 2025) further supports this design by enabling straightforward assembly and exchange of parts, giving the system a quasi-modular cloning property.

A key outcome of this study is the expansion of endogenous regulatory elements beyond the legumain module previously used for transgene expression in *Blastocystis* ST7-B (Li et al., 2018). This matters because a useful toolkit requires more than a single high-output cassette. Strong expression may be advantageous for selectable markers and bright reporters, but not for every cargo. Hence, weak or negligible promoter-terminator pairs may be useful for expressing toxic proteins or tightly regulated genes that would otherwise harm the host at high expression levels. The promoter-terminator combinations identified here therefore provide a practical expression

range for future reporter design and multi-gene constructs. At the same time, the screen highlights an important constraint on part discovery across *Blastocystis* subtypes. Candidate nomination based on *Blastocystis* ST4-WR1 protein abundance and a conserved 3' UTR motif provided a reasonable starting point, but these features were not sufficient to predict activity in *Blastocystis* ST7-B, as illustrated by the poor performance of the AAL-derived fragments. Cross-subtype information can therefore guide candidate selection but cannot substitute for direct validation in the subtype being engineered. The promoter length series further indicates that regulatory output in *Blastocystis* ST7-B is strongly context-dependent. Longer fragments did not consistently improve activity, arguing against simple length-based design rules and instead pointing to a more compact promoter organisation in which relatively small sequence differences can alter initiation efficiency or introduce inhibitory context (Li et al., 2017). Although the present constructs were not designed to define the regulatory architecture of these promoter regions directly, they point to a clear next step in dissecting this logic, including transcription start site mapping and refinement of promoter boundaries. A similar principle likely applies to 3' regions, where locus-specific cleavage and polyadenylation features may also contribute to the observed differences in expression.

A second important contribution of this study is the refinement of DNA delivery and recovery conditions for *Blastocystis* ST7-B. Electroporation in *Blastocystis* ST7-B appears to operate within a narrow window in which efficient DNA delivery must be balanced against cell survival and post-transfection recovery. Under the previously recommended time-constant settings at 370 V, arcing was frequent and cultures often failed during recovery. By contrast, the optimised square-wave settings avoided arcing and preserved enough viable cells to support post-transfection outgrowth. This distinction matters because successful transfection in *Blastocystis* ST7-B is not defined solely by DNA entry, but also by whether a sufficient number of cells survive to re-establish growth, a practical constraint consistent with the long-recognised but still poorly understood density-dependent growth behaviour of *Blastocystis* in liquid culture (Ho et al., 1993). Selection and clonal recovery then complete the transition from transient uptake to stable episomal line generation, and the present data indicate that this recovery phase is a major bottleneck. Immediate transfer into fully inhibitory drug concentrations caused culture collapse, whereas staged enrichment allowed resistant populations to emerge, indicating that stable episomal line generation depends as much on managing post-transfection stress as on drug potency itself. Among the selectable systems tested, puromycin and trimethoprim proved the most reliable in practice. WR99210 was initially attractive because of its established use in other protists and the presence of a putative DHFR-TS homologue in the *Blastocystis* ST7-B genome (Fidock and Wellems, 1997; Remcho et al., 2020), but its inconsistent behaviour across sources argues against routine use in *Blastocystis*. This result is informative because selectable markers that perform well in one protist cannot be assumed to transfer cleanly to another, and in toolkit development practical robustness matters more than theoretical compatibility. This vulnerable recovery phase also places a premium on careful culture handling. Bacterial contamination can readily compromise recovering *Blastocystis* cultures, making contamination control a practical part of workflow feasibility rather than a minor technical detail.

The P2A bicistronic design adds useful flexibility to the system by enabling two coding sequences to be expressed from a single transcriptional unit, for example a selectable marker paired with a reporter. In a platform where fully validated regulatory parts remain limited, this offers a practical way to simplify construct architecture while expanding design options. The present data show that P2A-based cassettes are functional in *Blastocystis* ST7-B and support coupled selection and transgene expression through recovery and colony expansion. However, the evidence presented here is functional rather than biochemical, so the efficiency of ribosomal skipping and the extent of any residual uncleaved product remain unresolved.

The reporter comparisons further show that fluorescent output in *Blastocystis* ST7-B is constrained by more than transgene expression alone, with each system exposing a different practical limitation. UnaG produced a clear signal in intact cells without oxygen-dependent chromophore maturation, which is a major advantage in an anaerobic protist (Kumagai et al.,

2013; Kwon et al., 2020). However, the fluorescence was compartmentalised despite the absence of an obvious targeting sequence, suggesting that signal distribution may be influenced by unconjugated BR availability or partitioning in addition to reporter localisation. This interpretation is plausible given the hydrophobic behaviour of unconjugated BR and its tendency to partition into lipid environments (Ostrow and Celic, 1984; Zucker et al., 1999; Bracken et al., 2024). UnaG is therefore functional in *Blastocystis* ST7-B, but appears less suitable for uniform whole-cell labelling or straightforward quantitative imaging across the cell. smURFP exposed a different constraint. Fluorescence was detectable only after saponin treatment, suggesting that limited chromophore access is likely the main barrier under the conditions tested (Rodriguez et al., 2016). This is consistent with the limited membrane permeability expected for BV and with the barrier properties attributed to the *Blastocystis* cell surface (Lightner et al., 1996; Bulmer et al., 2008; Yoshikawa and Hayakawa, 1996; Yason and Tan, 2018; Zheng and Gallot, 2020). In its current form, smURFP therefore appears better suited to permeabilised preparations than to straightforward live-cell imaging, although membrane-permeant bilins and newer monomeric variants may broaden its future utility (Hu et al., 2024; Maiti et al., 2023; Rodriguez et al., 2016). Among the reporters tested here, SNAP-tag® was the most adaptable in practice. Labelling worked in intact cells, signal scaled with substrate concentration, and the available chemistry provides access to a broad range of fluorophores and imaging modalities (Keppler et al., 2003; Gautier et al., 2008; Birke et al., 2022; Saimi and Chen, 2023; Porzberg et al., 2025). Although substrate-dependent labelling increases consumable cost, SNAP-tag® currently appears to offer the greatest practical versatility among the reporters evaluated here.

There are clear limitations to the present framework. Because all constructs were maintained episomally, copy number, segregation, and long-term expression stability remain unresolved, and these variables are likely to contribute to clone-to-clone heterogeneity, particularly where more quantitative readouts are required. The toolkit also remains limited to transgene expression and reporter validation, with targeted integration, conditional control, and direct loss-of-function approaches still to be established.

Conclusions

Taken together, this work establishes a practical framework for stable episomal transgenesis in *Blastocystis* ST7-B and extends the organism beyond the limited genetic tools available previously. By bringing endogenous regulatory part discovery, DNA delivery, selection, clonal recovery, and reporter validation into a single pipeline, it creates a flexible foundation for routine transgene-based studies in this system. In doing so, it shows that *Blastocystis* ST7-B can be genetically modified and that stable episomal transgenic lines can be generated, opening the way to more direct molecular analysis of its cell biology. More broadly, the strategy taken here provides a practical blueprint for developing genetic tools in other lesser understood microbial eukaryotes where genetic access remains limited.

Supplemetal Data 1

Supplemental Data 1. Gene sequences of reporter genes, selection markers, Kozak, and P2A linker

>JQ437370.1Nanoluc luciferase ATGGTCTTCACACTCGAAGATTTCGTTGGGGACTGGCGACAGACAGCC GGCTAC AACCTGGACCAAGTCCTTGAACAGGGAGGTGTGTCCAGTTTGTTTCAGAATCTC GGGGTGTCCGT AACTCCGATCCAAAGGATTGTCCTGAGCGGTGAAAATGGGCTG AAGATCGACATCCATGTCATCATCCCGTA TGAAGGTCTGAGCGGCGACCAAATG GGCCAGATCGAAAAAATTTTTAAGGTGGTGTACCCTGTGGATGATC ATCACTTTA AGGTGATCCTGCACTATGGCACACTGGTAATCGACGGGGTTACGCCGAACATGA TCGACTATT TCGGACGGCCGTATGAAGGCATCGCCGTGTTCGACGGCAAAAAGA TCACTGTAACAGGGACCCTGTGGAA CGGCAACAAAATTATCGACGAGCGCCTG ATCAACCCCGACGGCTCCCTGCTGTTCCGAGTAACCATCAACGG AGTGACCGGC TGGCGGCTGTGCGAACGCATTCTGGCGTAA

>smURFP *Blastocystis* ST7-B codon-optimized ATGGCTAAGACGTCGGAGCAGCGCGTGAACATTGCGAC GCTGCTGACGGAAAA CAAGAAAAAGATCGTGGATAAGGCGTCGCAGGATCTGTGGCGACGCCATCCGG AT CTGATTGCGCCTGGCGGAATCGCGTTCTCGCAGCGCGATCGAGCGCTGTGCCT GCGCGATTACGGATGGTT CCTGCACCTGATCACGTTCTGCCTGCTGGCTGGCGAT AAGGGACCGATCGAGTCGATTGGACTGATCTCGAT CCGCGAGATGTATAACTCG CTGGGAGTGCCGGTGCCTGCTATGATGGAATCGATCCGCTGCCTGAAAGAGG CG TCGCTGTCGCTGCTGGATGAGGAAGATGCGAACGAGACTGCGCCTTACTTCGAT TACATCATCAAGGCT ATGTCGTAA

>SNAP-tag *Blastocystis* ST7-B codon-optimized ATGGATAAGGATTGCGAGATGAAGCGCACGACGCTGG ATTCGCCTCTGGGAAAG CTGGAACTGTCGGGATGCGAGCAGGGACTGCACCGCATCATCTTTCTCGGAAAG GGAACGTCGGCTGCGGATGCGGTGGAAGTGCCTGCGCCTGCTGCTGTGCTCGGA GGACCTGAGCCTCTGAT GCAGGCGACGGCGTGGCTGAACGCGTACTTCCATCAG CCTGAGGCGATCGAGGAATTCCCGGTGCCTGCTC TGCACCATCCGGTGTTCCAG CAAGAGTCGTTCACGCGACAGGTGCTGTGGAAGCTGCTGAAGGTGGTGAAG TT CGGAGAGGTGATCTCGTACTCGCACCTGGCTGCGCTGGCTGGAAACCCTGCGGC TACGGCTGCGGTGAA AACGGCTCTGTCGGGAAACCCGGTGCCGATCCTGATTCC GTGCCACCGCGTGGTGCAGGGCGATCTGGATG TTGGAGGATACGAAGGCGGACT GGCGGTGAAAGAGTGGCTGCTGGCGCACGAGGGACACCGCCTCGGAA AGCCTG GACTGGGATAA

>UnaG *Blastocystis* ST7-B codon-optimized ATGGTCGAGAAGTTCGTTGGAACGTGGAAGATCGCGGATT CGCACAACTTCGGA GAGTACCTGAAGGCGATCGGAGCGCCTAAAGAACTGTCTGATGGCGGAGATGCT AC GACGCCGACGCTGTACATTTCGCAAAAGGATGGCGATAAGATGACCGTGAA GATCGAGAACGGACCGCCG ACCTTCCTGGATACGCAAGTGAAGTTCAAGCTGG GAGAAGAGTTCGATGAGTTCCCGTCGGATCGCCGAAA GGGCGTGAAGTCGGTG GTTAACCTCGTGGGAGAGAAGCTGGTGTACGTGCAGAAGTGGGACGGAAAAGA AACGACCTACGTGCGCGAGATCAAGGATGGAAAGCTGGTGGTTACGCTGACGAT GGGAGATGTGGTGGCT GTGCGATCGTATCGCCGAGCGACTGAATAA

>*E. coli* dhfr *Blastocystis* ST7-B codon-optimized ATGGAAAACGCTATGCCGTGGAACCTGCCTGCGGAT CTGGCGTGGTTCAAGCGC AACACGCTGAACAAGCCGGTGATCATGGGACGCCACACGTGGGAGTCGATCG G ACGCCCTCTGCCTGGACGCAAGAACATCATCCTGTCGTCGCAGCCTGGAACGGA TGACCGCGTGACGTGG GTGAAGTCGGTGGATGAGGCGATTGCGGCTTGCGGAG ATGTGCCCGAGATCATGGTGATCGGAGGCGGAC GCGTGTACGAGCAGTTCCTGC CGAAGGCGCAGAAGCTGTACCTGACGCACATCGATGCGGAGGTGGAAGG CGAT ACGCACTTCCCGGATTACGAGCCGGATGATTGGGAGAGCGTGTTCTCGGAGTTC CACGATGCGGATG CGCAGAACTCGCACTCGTACTGCTTCGAGATCCTGGAACGC CGATAA

>human DHFR *Blastocystis* ST7-B codon-optimized ATGCACGGATCGCTGAACTGCATCGTGGCGGTGTC GCAGAACATGGGAATCGGA AAGAACGGCGATTACCCGTGGCCTCCGCTGCGCAACGAGTTCCGCTACTTCC AG CGCATGACGACGACGTCGAGCGTGGAAGGCAAGCAGAACCTGGTGATCATGGG AAAGAAAACGTGGT TCTCGATCCCCGAGAAGAATCGCCCTCTGAAGGGACGCA TCAACCTGGTGCTGTCGCGAGAGCTGAAAGAA CCGCCTCAGGGTGCGCACTTCC TGTCGCGCTCGCTGGATGATGCGCTGAAGCTGACGGAACAGCCCGAGCT GGCG AACAAGGTGGATATGGTGTGGATCGTTGGAGGATCGTCGGTGTACAAAGAAGCT ATGAACCATCCG GGACACCTGAAGCTGTTCGTGACGCGCATCATGCAGGATTTC GAGTCGGATACGTTCTTCCCCGAGATCGAC CTGGAAAAGTACAAGCTGCTGCCT GAGTACCCTGGCGTGCTGTCGGATGTGCAAGAGGAAAAGGGAATCA AGTACAA GTTCGAGGTGTACGAGAAGAACGACTAA

>pac *Blastocystis* ST7-B codon-optimized ATGACCGAGTACAAGCCTACTGTGCGACTGGCGACGCGAGAT GATGTTCCTAGA GCTGTGCGAACGCTGGCGGCTGCGTTTGCTGATTATCCTGCTACGCGCCACACGG TGGA TCCTGATCGCCATATTGAACGCGTGACGGAACTGCAAGAGCTGTTCCTGA CGCGCGTGGGACTCGATATCG GAAAAGTGTGGGTTGCCGATGATGGCGCTGCTG TGGCTGTGTGGACTACGCCTGAATCTGTGGAAGCGGG TGCTGTGTTCGCGGAGA TTGGACCTAGAATGGCGGAACTGTCTGGATCTAGACTGGCGGCGCAGCAGCAG A TGGAAGGACTTTTGGCGCCGCACCGACCTAAAGAACCTGCTTGGTTTCTGGCGA CCGTGGGAGTGTCTCC GGATCACCAAGGCAAAGGATTGGGATCTGCTGTGGTGC TGCCTGGCGTTGAAGCTGCTGAACGAGCTGGT GTTCCGGCTTTCTTGGAAACGTC GGCGCCTCGCAACCTGCCTTTCTATGAACGCCTGGGATTCACCGTGACG GCGGA TGTGGAAGTTCCTGAAGGACCTCGAACGTGGTGCATGACGCGCAAGCCTGGTGC TTAA

>P2A sequence *Blastocystis* ST7-B codon-optimized GGCAGCGGAGCGACGAACTTCTCGCTGCTGAAGC AGGCTGGCGACGTGGAAGA GAACCCTGGACCG

Primer/ssOB	Sequence (5' to 3')
pMRT_AATpro-1000	
MRT-75	TCATGGATCGAATTGCTTCCATC
MRT-76	TGTATAGAATCAATAGAAATCTATATGAAACAGGAG
MRT-77	GCCATTTGAATTCATGGTTGTTTCAATTAC
MRT-78	TATTTGGACTCGCGCGCG
ssOB_18	TTTCATATAGATTTCTATTGATTCTATACAATGGTCTTCACACTCGAAGATTTCGTTGGG
ssOB_20	CACGACGTTGTAAAACGACGGCCAGTGCCATCATGGATCGAATTGCTTCCATCAGACGTA
ssOB_21	TGGCGGCTGTGCGAACGCATTCTGGCGTAAGCCATTTGAATTCATGGTTGTTTCAATTAC
ssOB_22	CAACACGTCCGTCGCGCGCGAGTCCAAATAAATTCGTAATCATGGTCATAGCTGTTTCCT
pMRT_AATpro-1500	
MRT-74	GGGTTGACATAGGGGATTCTTGTC
MRT-76	TGTATAGAATCAATAGAAATCTATATGAAACAGGAG
MRT-77	GCCATTTGAATTCATGGTTGTTTCAATTAC
MRT-78	TATTTGGACTCGCGCGCG
ssOB_18	TTTCATATAGATTTCTATTGATTCTATACAATGGTCTTCACACTCGAAGATTTCGTTGGG
ssOB_19	CACGACGTTGTAAAACGACGGCCAGTGCCAGGGTTGACATAGGGGATTCTTGTCTGGAAG
ssOB_21	TGGCGGCTGTGCGAACGCATTCTGGCGTAAGCCATTTGAATTCATGGTTGTTTCAATTAC
ssOB_22	CAACACGTCCGTCGCGCGCGAGTCCAAATAAATTCGTAATCATGGTCATAGCTGTTTCCT
pMRT_AATpro-2438	
MRT-73	TAAGCGAATAAAATGATATGTATTAATACCTACCATAG
MRT-76	TGTATAGAATCAATAGAAATCTATATGAAACAGGAG
MRT-77	GCCATTTGAATTCATGGTTGTTTCAATTAC
MRT-78	TATTTGGACTCGCGCGCG
ssOB_17	CACGACGTTGTAAAACGACGGCCAGTGCCATAAGCGAATAAAATGATATGTATTAATACC
ssOB_18	TTTCATATAGATTTCTATTGATTCTATACAATGGTCTTCACACTCGAAGATTTCGTTGGG
ssOB_21	TGGCGGCTGTGCGAACGCATTCTGGCGTAAGCCATTTGAATTCATGGTTGTTTCAATTAC
ssOB_22	CAACACGTCCGTCGCGCGCGAGTCCAAATAAATTCGTAATCATGGTCATAGCTGTTTCCT
pMRT_40SRPS7pro-1000	
MRT-64	ACTTCCTTTTACCCGATTTAGCATTGAAG
MRT-65	GGTCTACACAACGAATTAGCGAC
MRT-66	GAAAGTCGATACTTGAGGGTGGG
MRT-67	ACAAAGTAAAATCGGTACTTTTCGTAGATG
ssOB_1	CACGACGTTGTAAAACGACGGCCAGTGCCAACTTCCTTTTACCCGATTTAGCATTGAAGC
ssOB_2	TCGAATAGTCGCTAATTCGTTGTGTAGACCATGGTCTTCACACTCGAAGATTTCGTTGGG

Supplemental Table 1. Oligonucleotide sets used for expression vector cloning.

In cases where only the promoter fragment was changed, most oligonucleotides were reused; however, complete sets are shown here for clarity and completeness. Primers used for PCR amplification of DNA fragments are designated MRT-*xxx*, whereas single-stranded oligonucleotide bridges used for DNA assembly are termed ssOB-*yyy*. Oligonucleotides are grouped by plasmid, named pMRT-*zzz*.

ssOB_5	TGGCGGCTGTGCGAACGCATTCTGGCGTAAGAAAGTCGATACTTGAGGGTGGGTTATACT
ssOB_6	CATCTACGAAAAGTACCGATTTTACTTTGTAATTCGTAATCATGGTCATAGCTGTTTCCT
pMRT_40SRPS7pro-1500	
MRT-63	AGATAGAAATCCAAATTCTGAGCACAGC
MRT-65	GGTCTACACAACGAATTAGCGAC
MRT-66	GAAAGTCGATACTTGAGGGTGGG
MRT-67	ACAAAGTAAAATCGGTACTTTTCGTAGATG
ssOB_2	TCGAATAGTCGCTAATTCGTTGTGTAGACCATGGTCTTCACACTCGAAGATTTCGTTGGG
ssOB_3	CACGACGTTGTAAAACGACGGCCAGTGCCAAGATAGAAATCCAAATTCTGAGCACAGCGC
ssOB_5	TGGCGGCTGTGCGAACGCATTCTGGCGTAAGAAAGTCGATACTTGAGGGTGGGTTATACT
ssOB_6	CATCTACGAAAAGTACCGATTTTACTTTGTAATTCGTAATCATGGTCATAGCTGTTTCCT
pMRT_40SRPS7pro-2041	
MRT-62	CGAAGCCAAGAAAAATGGAACCAAAATC
MRT-65	GGTCTACACAACGAATTAGCGAC
MRT-66	GAAAGTCGATACTTGAGGGTGGG
MRT-67	ACAAAGTAAAATCGGTACTTTTCGTAGATG
ssOB_2	TCGAATAGTCGCTAATTCGTTGTGTAGACCATGGTCTTCACACTCGAAGATTTCGTTGGG
ssOB_4	CACGACGTTGTAAAACGACGGCCAGTGCCACGAAGCCAAGAAAAATGGAACCAAAATCAC
ssOB_5	TGGCGGCTGTGCGAACGCATTCTGGCGTAAGAAAGTCGATACTTGAGGGTGGGTTATACT
ssOB_6	CATCTACGAAAAGTACCGATTTTACTTTGTAATTCGTAATCATGGTCATAGCTGTTTCCT
pMRT_60SRPL3pro-500	
MRT-69	AATGACAAAATTCACGCCTTCAACCAG
MRT-70	GCTGTTTGATTAGGAAAAAAGTGAGG
MRT-71	GAGAGTCGAACGATCGATTGGGAAAT
MRT-72	TTTTAAATTGTTTTTTGTGTCCTTCATGC
ssOB_7	CACGACGTTGTAAAACGACGGCCAGTGCCAAATGACAAAATTCACGCCTTCAACCAGAAC
ssOB_8	TTTTCCTCACTTTTTTCCTAATCAAACAGCATGGTCTTCACACTCGAAGATTTCGTTGGG
ssOB_10	AGCATGAAGGACACAAAAAACAATTTAAAAAATTCGTAATCATGGTCATAGCTGTTTCCT
ssOB_11	TGGCGGCTGTGCGAACGCATTCTGGCGTAAGAGAGTCGAACGATCGATTGGGAAATAATT
pMRT_60SRPL3pro-1000	
MRT-68	ACAGACAGCTAGCTAGGTCATTCA
MRT-70	GCTGTTTGATTAGGAAAAAAGTGAGG
MRT-71	GAGAGTCGAACGATCGATTGGGAAAT
MRT-72	TTTTAAATTGTTTTTTGTGTCCTTCATGC
ssOB_8	TTTTCCTCACTTTTTTCCTAATCAAACAGCATGGTCTTCACACTCGAAGATTTCGTTGGG
ssOB_9	CACGACGTTGTAAAACGACGGCCAGTGCCAACAGACAGCTAGCTAGGTCATTCAGAATGG
ssOB_10	AGCATGAAGGACACAAAAAACAATTTAAAAAATTCGTAATCATGGTCATAGCTGTTTCCT
ssOB_11	TGGCGGCTGTGCGAACGCATTCTGGCGTAAGAGAGTCGAACGATCGATTGGGAAATAATT
pMRT_AALpro-1000	
MRT-80	CACGCAAACGCACCCAGC
MRT-81	TTTCAAGATAAGGGCAAAGAAAAAATATGATTTTC
MRT-82	AGAGAAGAGAAGGGATTGGGAAG
MRT-83	GAAATCGAGTTGAGGCTTCAGG
ssOB_12	CACGACGTTGTAAAACGACGGCCAGTGCCACACGCAAACGCACCCAGCACTGTTGCACGA

Supplemental Table 1. (continued)

ssOB_13	TCATATTTTTTCTTTGCCCTTATCTTGAAAATGGTCTTCACACTCGAAGATTTCGTTGGG
ssOB_15	TGGCGGCTGTGCGAACGCATTCTGGCGTAAAGAGAAGAGAAGGGATTGGGAAGAGTGCTG
ssOB_16	CTCCAAGTCCTGAAGCCTCAACTCGATTTCAATTCGTAATCATGGTCATAGCTGTTTCCT
pMRT_AALpro-1500	
MRT-79	TCGATATTCTTCCCACATGTGATTTTC
MRT-81	TTTCAAGATAAGGGCAAAGAAAAAATATGATTTTC
MRT-82	AGAGAAGAGAAGGGATTGGGAAG
MRT-83	GAAATCGAGTTGAGGCTTCAGG
ssOB_13	TCATATTTTTTCTTTGCCCTTATCTTGAAAATGGTCTTCACACTCGAAGATTTCGTTGGG
ssOB_14	CACGACGTTGTAAAACGACGGCCAGTGCCATCGATATTCTTCCCACATGTGATTTTCTTT
ssOB_15	TGGCGGCTGTGCGAACGCATTCTGGCGTAAAGAGAAGAGAAGGGATTGGGAAGAGTGCTG
ssOB_16	CTCCAAGTCCTGAAGCCTCAACTCGATTTCAATTCGTAATCATGGTCATAGCTGTTTCCT
pMRT_CathB2pro-500	
MRT-90	CAACGGTCCTATTGAGGTCGATTTC
MRT-91	ATTTACTTACTAAATATTTTCTGGGAAAGAGGATAAC
MRT-92	GGTGTTCTTCTGGTTGGTTTGTTTG
MRT-93	TCCTCCCTACAAGGAAAGCG
ssOB_33	CACGACGTTGTAAAACGACGGCCAGTGCCACAACGGTCCTATTGAGGTCGATTTCTCTGT
ssOB_34	TCTTTCCCAGAAAATATTTAGTAAGTAAATATGGTCTTCACACTCGAAGATTTCGTTGGG
ssOB_36	TGGCGGCTGTGCGAACGCATTCTGGCGTAAGGTGTTCTTCTGGTTGGTTTGTTTGTTTGA
ssOB_37	ACGTGAACATCGCTTTCCTTGTAGGGAGGAAATTCGTAATCATGGTCATAGCTGTTTCCT
pMRT_CathB2pro-1000	
MRT-89	GGTGATCTTCCTGAGTCTTTCGAC
MRT-91	ATTTACTTACTAAATATTTTCTGGGAAAGAGGATAAC
MRT-92	GGTGTTCTTCTGGTTGGTTTGTTTG
MRT-93	TCCTCCCTACAAGGAAAGCG
ssOB_34	TCTTTCCCAGAAAATATTTAGTAAGTAAATATGGTCTTCACACTCGAAGATTTCGTTGGG
ssOB_35	CACGACGTTGTAAAACGACGGCCAGTGCCAGGTGATCTTCCTGAGTCTTTCGACCCCGTG
ssOB_36	TGGCGGCTGTGCGAACGCATTCTGGCGTAAGGTGTTCTTCTGGTTGGTTTGTTTGTTTGA
ssOB_37	ACGTGAACATCGCTTTCCTTGTAGGGAGGAAATTCGTAATCATGGTCATAGCTGTTTCCT
pMRT_CBMCPpro-378	
MRT-85	GTTTGAGATGCTTGGGGCG
MRT-86	TCAAGTATAATTTCAAATCTCATTCATTTCTGAATC
MRT-87	ACACTGATTGGTGTTGTGACAATATTTATTTATTTATTTG
MRT-88	CACACGCGATAAAGACGAATCAATTC
ssOB_38	CACGACGTTGTAAAACGACGGCCAGTGCCAGTTTGAGATGCTTGGGGCGCTTATTGTGTA
ssOB_39	GAAATGAATGAGATTTGAAATTATACTTGAATGGTCTTCACACTCGAAGATTTCGTTGGG
ssOB_41	TGGCGGCTGTGCGAACGCATTCTGGCGTAAACACTGATTGGTGTTGTGACAATATTTATT
ssOB_42	GAACGAATTGATTCGTCTTTATCGCGTGTGAATTCGTAATCATGGTCATAGCTGTTTCCT
pMRT_CBMCPpro-572	
MRT-84	GTAGCAGATTCTTTGGTAGGTTCATC
MRT-86	TCAAGTATAATTTCAAATCTCATTCATTTCTGAATC
MRT-87	ACACTGATTGGTGTTGTGACAATATTTATTTATTTATTTG
MRT-88	CACACGCGATAAAGACGAATCAATTC

Supplemental Table 1. (continued)

ssOB_39	GAAATGAATGAGATTTGAAATTATACTTGAATGGTCTTCACACTCGAAGATTTCGTTGGG
ssOB_40	CACGACGTTGTAAAACGACGGCCAGTGCCAGTAGCAGATTCTTTGGTAGGTTCATCCTAG
ssOB_41	TGGCGGCTGTGCGAACGCATTCTGGCGTAAACACTGATTGGTGTTGTGACAATATTTATT
ssOB_42	GAACGAATTGATTCGTCTTTATCGCGTGTGAATTCGTAATCATGGTCATAGCTGTTTCCT
pMRT_EamApro-1023	
MRT-95	GTATGGAATGCGATGGAGTGTTC
MRT-96	TCTAGAGAATGAACTATTCTAGATTTCACCATAC
MRT-97	TGGTAGTGTTGCGTTTGTTAGAAAC
MRT-98	CACCAAATCCCAAATCTCTTTACGC
ssOB_43	CACGACGTTGTAAAACGACGGCCAGTGCCAGTATGGAATGCGATGGAGTGTTCTCTCTCT
ssOB_44	GGTGAAATCTAGAATAGTTCATTCTCTAGAATGGTCTTCACACTCGAAGATTTCGTTGGG
ssOB_46	TGGCGGCTGTGCGAACGCATTCTGGCGTAATGGTAGTGTTGCGTTTGTTAGAAACACGTT
ssOB_47	AAGCAGCGTAAAGAGATTTGGGATTTGGTGAATTCGTAATCATGGTCATAGCTGTTTCCT
pMRT_EamApro-1245	
MRT-94	GTAAGTTTCTTTCTAGAAGTAGAGTTGATCG
MRT-96	TCTAGAGAATGAACTATTCTAGATTTCACCATAC
MRT-97	TGGTAGTGTTGCGTTTGTTAGAAAC
MRT-98	CACCAAATCCCAAATCTCTTTACGC
ssOB_44	GGTGAAATCTAGAATAGTTCATTCTCTAGAATGGTCTTCACACTCGAAGATTTCGTTGGG
ssOB_45	CACGACGTTGTAAAACGACGGCCAGTGCCAGTAAGTTTCTTTCTAGAAGTAGAGTTGATC
ssOB_46	TGGCGGCTGTGCGAACGCATTCTGGCGTAATGGTAGTGTTGCGTTTGTTAGAAACACGTT
ssOB_47	AAGCAGCGTAAAGAGATTTGGGATTTGGTGAATTCGTAATCATGGTCATAGCTGTTTCCT
pMRT_GDHpro-1500	
MRT-99	GGCAACAATTTCTGCAAGATGAAG
MRT-101	CTATGTGATCAGAGCGGGACG
MRT-102	TCAACCAACCAACCAACCG
MRT-103	TGGGAGGAGCGAGGAGTAG
ssOB_49	TGTTGTCGGCGTCCCGCTCTGATCACATAGATGGTCTTCACACTCGAAGATTTCGTTGGG
ssOB_50	CACGACGTTGTAAAACGACGGCCAGTGCCAGGCAACAATTTCTGCAAGATGAAGGAGGTG
ssOB_51	TGGCGGCTGTGCGAACGCATTCTGGCGTAATCAACCAACCAACCAACCGCTTCCTTCCTG
ssOB_52	CACATCAGAATCTACTCCTCGCTCCTCCCAAATTCGTAATCATGGTCATAGCTGTTTCCT
pMRT_G/M_MDHpro-1000	
MRT-105	ATGACAACGAAATAAACGTAATGTAAGAGAAAAG
MRT-106	ATGAAAAGAAAATATTTTGCTAGATATCAATTTGTAGAAAC
MRT-107	ATCGTAATAGTTTTGGTTATGTTTTTTGAATGTTTG
MRT-108	GAGAGAACAGTACTGTGCTAAAAATCAAG
ssOB_53	CACGACGTTGTAAAACGACGGCCAGTGCCAATGACAACGAAATAAACGTAATGTAAGAGA
ssOB_54	TTGATATCTAGCAAAATATTTTCTTTTCATATGGTCTTCACACTCGAAGATTTCGTTGGG
ssOB_56	TGGCGGCTGTGCGAACGCATTCTGGCGTAAATCGTAATAGTTTTGGTTATGTTTTTTGAA
ssOB_57	TCTTGATTTTTAGCACAGTACTGTTCTCTCAATTCGTAATCATGGTCATAGCTGTTTCCT
pMRT_G/M_MDHpro-1500	
MRT-104	AGTGGGGAATGTCGGCACTTTTC
MRT-106	ATGAAAAGAAAATATTTTGCTAGATATCAATTTGTAGAAAC
MRT-107	ATCGTAATAGTTTTGGTTATGTTTTTTGAATGTTTG

Supplemental Table 1. (continued)

MRT-108	GAGAGAACAGTACTGTGCTAAAAATCAAG
ssOB_54	TTGATATCTAGCAAAATATTTTCTTTTCATATGGTCTTCACACTCGAAGATTTCGTTGGG
ssOB_55	CACGACGTTGTAAAACGACGGCCAGTGCCAAGTGGGGAATGTCGGCACTTTTCTAAATGA
ssOB_56	TGGCGGCTGTGCGAACGCATTCTGGCGTAAATCGTAATAGTTTTGGTTATGTTTTTTGAA
ssOB_57	TCTTGATTTTTAGCACAGTACTGTTCTCTCAATTCGTAATCATGGTCATAGCTGTTTCCT
pMRT_MPTpro-903	
MRT-110	TCGGGTAGATATCCGAAAACGAAG
MRT-111	TTGGAGAAATAAGTATGAGGGATCTAGG
MRT-112	GTGTTTTTCTTTTTGAATAATAACGTAACTAAATGA
MRT-113	CTAGTAATAACCTCAAATAGTCTTGTGCATTAC
ssOB_58	CACGACGTTGTAAAACGACGGCCAGTGCCATCGGGTAGATATCCGAAAACGAAGATTTAC
ssOB_59	TTCCTAGATCCCTCATACTTATTTCTCCAAATGGTCTTCACACTCGAAGATTTCGTTGGG
ssOB_61	TGGCGGCTGTGCGAACGCATTCTGGCGTAAGTGTTTTTCTTTTTGAATAATAACGTAACT
ssOB_62	ATGCACAAGACTATTTGAGGTTATTACTAGAATTCGTAATCATGGTCATAGCTGTTTCCT
pMRT_MPTpro-1688	
MRT-109	GTGTGTTTGGAATGTCCGGAC
MRT-111	TTGGAGAAATAAGTATGAGGGATCTAGG
MRT-112	GTGTTTTTCTTTTTGAATAATAACGTAACTAAATGA
MRT-113	CTAGTAATAACCTCAAATAGTCTTGTGCATTAC
ssOB_60	TTCCTAGATCCCTCATACTTATTTCTCCAAATGGTCTTCACACTCGAAGATTTCGTTGGG
ssOB_59	TTCCTAGATCCCTCATACTTATTTCTCCAAATGGTCTTCACACTCGAAGATTTCGTTGGG
ssOB_61	TGGCGGCTGTGCGAACGCATTCTGGCGTAAGTGTTTTTCTTTTTGAATAATAACGTAACT
ssOB_62	ATGCACAAGACTATTTGAGGTTATTACTAGAATTCGTAATCATGGTCATAGCTGTTTCCT
pMRT_SARFGBPpro-600	
MRT-114	CGAACGATAAGGCTCGTATTGAG
MRT-116	CTATACAAAACTGTTAGATATAAGCTCTATATTGATATATTTG
MRT-117	AGTGATTTGAACTAATAGAAATAGCGTTTG
MRT-118	AGTCCACAGTCTCCACATTAAATCC
ssOB_64	CCCCAACGAAATCTTCGAGTGTGAAGACCATCTATACAAAACTGTTAGATATAAGCTCTAT
ssOB_65	CACGACGTTGTAAAACGACGGCCAGTGCCACGAACGATAAGGCTCGTATTGAGGATGCTA
ssOB_68	TGGCGGCTGTGCGAACGCATTCTGGCGTAAAGTGATTTGAACTAATAGAAATAGCGTTTG
ssOB_69	G69CATTGGATTTAATGTGGAGACTGTGGACTAATTCGTAATCATGGTCATAGCTGTTTCCT
pMRT_SARFGBPpro-600	
MRT-117	AGTGATTTGAACTAATAGAAATAGCGTTTG
MRT-118	AGTCCACAGTCTCCACATTAAATCC
MRT-123	TTCTCGATAGAATCTAGTTGAAAGAGAAAATTG
MRT-124	CTATACAAAACTGTTAGATATGAACTCTATATTGATATATTTG
ssOB_66	CACGACGTTGTAAAACGACGGCCAGTGCCATTCTCGATAGAATCTAGTTGAAAGAGAAAA
ssOB_67	ATAGAGTTCATATCTAACAGTTTTGTATAGATGGTCTTCACACTCGAAGATTTCGTTGGG
ssOB_68	TGGCGGCTGTGCGAACGCATTCTGGCGTAAAGTGATTTGAACTAATAGAAATAGCGTTTG
ssOB_69	G69CATTGGATTTAATGTGGAGACTGTGGACTAATTCGTAATCATGGTCATAGCTGTTTCCT
pMRT_LeguP1:UnaG::P2A::pac:Legu3′UTR	
MRT-4	GCTAGCTTACAAATTTTTTATGGTATTATTTCTAC
MRT-5	GGATCCGCATTGAGTGTATATGTTTG

Supplemental Table 1. (continued)

MRT-159	ACTTTGTACAAAAAAGCAGGCTTCGC
MRT-160	TTCAGTCGCTCGGCGATACG
MRT-165	ATGACCGAGTACAAGCCTACTGTG
MRT-166	TTAAGCACCAGGCTTGCGC
ssOB_81	AATAATACCATAAAAAATTTGTAAGCTAGCACTTTGTACAAAAAAGCAGGCTTCGCCACC
ssOB_82	GCTGTGCGATCGTATCGCCGAGCGACTGAAGGCAGCGGAGCGACGAACTTCTCGCTGCTGAAGC AGGCTGGCGACGTGGA
ssOB_94	TGGTGCATGACGCGCAAGCCTGGTGCTTAAGGATCCGCATTGAGTGTATATGTTTGTTAT
ssOB_95	CAGTCGCACAGTAGGCTTGTACTCGGTCATCGGTCCAGGGTTCTCTTCCACGTCGCCAGCCTGCTT CAGCAGCGAG
pMRT_LeguP1:smURFP::P2A::Ecdhfr:Legu3'UTR	
MRT-4	GCTAGCTTACAAATTTTTTATGGTATTATTTCTAC
MRT-5	GGATCCGCATTGAGTGTATATGTTTG
MRT-159	ACTTTGTACAAAAAAGCAGGCTTCGC
MRT-161	ATGGAAAACGCTATGCCGTGGAAC
MRT-162	TTATCGGCGTTCCAGGATCTCGAAG
MRT-267	CGACATAGCCTTGATGATGTAATCGAAGTAAG
ssOB_81	AATAATACCATAAAAAATTTGTAAGCTAGCACTTTGTACAAAAAAGCAGGCTTCGCCACC
ssOB_85	CTGCTTCGAGATCCTGGAACGCCGATAAGGATCCGCATTGAGTGTATATGTTTGTTATAA
ssOB_86	AGGCAGGTTCCACGGCATAGCGTTTTCCATCGGTCCAGGGTTCTCTTCCACGTCGCCAG CCTGCTTCAGCAGCGAG
ssOB_165	TACTTCGATTACATCATCAAGGCTATGTCGGGCAGCGGAGCGACGAACTTCTCGCTGCTG
pMRT_LeguP1:SNAPtag::P2A::pac:Legu3'UTR	
MRT-4	GCTAGCTTACAAATTTTTTATGGTATTATTTCTAC
MRT-5	GGATCCGCATTGAGTGTATATGTTTG
MRT-159	ACTTTGTACAAAAAAGCAGGCTTCGC
MRT-165	ATGACCGAGTACAAGCCTACTGTG
MRT-166	TTAAGCACCAGGCTTGCGC
MRT-167	ACATGAACAGAATAATCCAGAACGAGGAAC
ssOB_81	AATAATACCATAAAAAATTTGTAAGCTAGCACTTTGTACAAAAAAGCAGGCTTCGCCACC
ssOB_94	TGGTGCATGACGCGCAAGCCTGGTGCTTAAGGATCCGCATTGAGTGTATATGTTTGTTAT
ssOB_95	CAGTCGCACAGTAGGCTTGTACTCGGTCATCGGTCCAGGGTTCTCTTCCACGTCGCCAGC CTGCTTCAGCAGCGAG
ssOB_167	GGACACCGCCTCGGAAAGCCTGGACTGGGAGGCAGCGGAGCGACGAACTTCTCGCTGCTG

Supplemental Table 1. (continued)

Data availability

Proteomic dataset used in this study was generated and published by Armengaud et al., 2017.

Acknowledgements

MRT was supported by Norwegian Research Council grant 301170 to MvdG. We thank Ms. Geok Choo Ng and Dr. Steven Santino Leonardi for generously sharing their wet-lab techniques for culturing *Blastocystis.* We thank Dr. Yohannes Seyoum for helping with the statistical analyses. We also thank Luz Aurora Martinez-Contreras, Daniel Simon Nagel, and Ayanara Mae Sadi Bukneberg for their help in routine culturing and maintenance of *Blastocystis* cultures.

Additional information

Author contributions

Conceptualisation and design of the research: MRT and MvdG

Critical advise: MvdG and KSWT

Experimental work and data analyses: MRT

Writing and editing: MRT, MvdG, and KSWT

All authors read and revised the paper.

Funding

Funder	Grant reference number	Author
Norges Forskningsråd (Forskningsrådet)	301170	M Rey Toleco Mark van der Giezen

Author ORCID iDs

Mark van der Giezen: https://orcid.org/0000-0002-1033-1335

References

Abrahamian M, Kagda M, Ah-Fong AMV, Judelson HS (2017) Rethinking the evolution of eukaryotic metabolism: novel cellular partitioning of enzymes in stramenopiles links serine biosynthesis to glycolysis in mitochondria. *BMC Evol Biol* **17**:241 https://doi.org/10.1186/s12862-017-1087-8 | PubMed

Alfellani MA, Stensvold CR, Vidal-Lapiedra A, Onuoha ESU, Fagbenro-Beyioku AF, Clark CG (2013) Variable geographic distribution of *Blastocystis* subtypes and its potential implications. *Acta Tropica* **126**:11-18 https://doi.org/10.1016/j.actatropica.2012.12.011 | PubMed

Altschul SF, Gish W, Miller W, Myers EW, Lipman DJ (1990) Basic local alignment search tool. *Journal of Molecular Biology* **215**:403-410 https://doi.org/10.1016/S0022-2836(05)80360-2 | PubMed

Armengaud J, Pible O, Gaillard J-C, Cian A, Gantois N, Tan KSW, Chabé M, Viscogliosi E (2017) Proteogenomic insights into the intestinal parasite *Blastocystis* sp. subtype 4 isolate WR1. *Proteomics* **17**:1700211 https://doi.org/10.1002/pmic.201700211 | PubMed

Asselbergs FAM, Widmer R (1995) Use of the *Escherichia coli* chromosomal DHFR gene as selection marker in mammalian cells. *Journal of Biotechnology* **43**:133-138 https://doi.org/10.1016/0168-1656(95)00131-3 | PubMed

Bártulos CR, Rogers MB, Williams TA, Gentekaki E, Brinkmann H, Cerff R, Liaud M-F, Hehl AB, Yarlett NR, Gruber A, *et al.* (2018) Mitochondrial glycolysis in a major lineage of eukaryotes. *Genome Biol and Evol* **10**:2310-2325 https://doi.org/10.1093/gbe/evy164 | PubMed

(2025) Benchling. https://benchling.com

Birke R, Ast J, Roosen DA, Lee J, Roßmann K, Huhn C, Mathes B, Lisurek M, Bushiri D, Sun H, *et al.* (2022) Sulfonated red and far-red rhodamines to visualize SNAP- and Halo-tagged cell surface proteins. *Org Biomol Chem* **20**:5967-5980 https://doi.org/10.1039/d1ob02216d | PubMed

Bracken ML, Fernandes MA, Mathura S (2024) Bilirubin and its crystal forms. *CrystEngComm* **26**:2136-2142 https://doi.org/10.1039/D4CE00123K

Bulmer AC, Blanchfield JT, Coombes JS, Toth I. (2008) *In vitro* permeability and metabolic stability of bile pigments and the effects of hydrophilic and lipophilic modification of biliverdin. *Bioorg Med Chem* **16**:3616-3625 https://doi.org/10.1016/j.bmc.2008.02.008 | PubMed

Camacho C, Coulouris G, Avagyan V, Ma N, Papadopoulos J, Bealer K, Madden TL (2009) BLAST+: architecture and applications. *BMC Bioinformatics* **10**:421 https://doi.org/10.1186/1471-2105-10-421 | PubMed

Chen XQ, Singh M, Ho LC, Tan SW, Ng GC, Moe KT, Yap EH (1997) Description of a *Blastocystis* species from *Rattus norvegicus*. *Parasitology Research* **83**:313-318 https://doi.org/10.1007/s004360050255 | PubMed

Deng L, Tan KSW (2025) From parasite to partner: unravelling the multifaceted role of *Blastocystis* in human health and disease. *The Lancet Microbe* **101155** https://doi.org/10.1016/j.lanmic.2025.101155 | PubMed

Deng L, Tan KSW (2022) Interactions between *Blastocystis* subtype ST4 and gut microbiota *in vitro*. *Parasites Vectors* **15**:80 https://doi.org/10.1186/s13071-022-05194-x | PubMed

Fidock DA, Wellems TE (1997) Transformation with human dihydrofolate reductase renders malaria parasites insensitive to WR99210 but does not affect the intrinsic activity of proguanil. *Proc Natl Acad Sci U S A* **94**:10931-10936 https://doi.org/10.1073/pnas.94.20.10931 | PubMed

Gautier A, Juillerat A, Heinis C, Corrêa IR, Kindermann M, Beaufils F, Johnsson K. (2008) An engineered protein tag for multiprotein labeling in living cells. *Chem Biol* **15**:128-136 https://doi.org/10.1016/j.chembiol.2008.01.007 | PubMed

Gentekaki E, Curtis BA, Stairs CW, Klimeš V, Eliáš M, Salas-Leiva DE, Herman EK, Eme L, Arias MC, Henrissat B, *et al.* (2017) Extreme genome diversity in the hyper-prevalent parasitic eukaryote *Blastocystis*. *PLoS Biol* **15**:e2003769 https://doi.org/10.1371/journal.pbio.2003769 | PubMed

Ho LC, Singh M, Suresh G, Ng GC, Yap EH (1993) Axenic culture of *Blastocystis hominis* in Iscove's modified Dulbecco's medium. *Parasitol Res* **79**:614-616 https://doi.org/10.1007/BF00932249 | PubMed

Hu X, Xu Y, Yi J, Wang C, Zhu Z, Yue T, Zhang H, Wang X, Wu F, Xue L, *et al.* (2024) Using protein design and directed evolution to monomerize a bright near-infrared fluorescent protein. *ACS Synth Biol* **13**:1177-1190 https://doi.org/10.1021/acssynbio.3c00643 | PubMed

Keppler A, Gendreizig S, Gronemeyer T, Pick H, Vogel H, Johnsson K (2003) A general method for the covalent labeling of fusion proteins with small molecules *in vivo*. *Nat Biotechnol* **21**:86-89 https://doi.org/10.1038/nbt765 | PubMed

Klimeš V, Gentekaki E, Roger AJ, Eliáš M (2014) A large number of nuclear genes in the human parasite *Blastocystis* require mRNA polyadenylation to create functional termination codons. *Genome Biology and Evolution* **6**:1956-1961 https://doi.org/10.1093/gbe/evu146 | PubMed

Koehler AV, Herath HMPD, Hall RS, Wilcox S, Gasser RB (2024) Marked genetic diversity within *Blastocystis* in Australian wildlife revealed using a next generation sequencing–phylogenetic approach. *International Journal for Parasitology: Parasites and Wildlife* **23**:100902 https://doi.org/10.1016/j.ijppaw.2023.100902 | PubMed

Kumagai A, Ando R, Miyatake H, Greimel P, Kobayashi T, Hirabayashi Y, Shimogori T, Miyawaki A (2013) A bilirubin-inducible fluorescent protein from eel muscle. *Cell* **153**:1602-1611 https://doi.org/10.1016/j.cell.2013.05.038 | PubMed

Kwon J, Park J-S, Kang M, Choi S, Park J, Kim GT, Lee C, Cha S, Rhee H-W, Shim S-H (2020) Bright ligand-activatable fluorescent protein for high-quality multicolor live-cell super-resolution microscopy. *Nat Commun* **11**:273 https://doi.org/10.1038/s41467-019-14067-4 | PubMed

Li F-J, Tsaousis AD, Purton T, Chow VTK, He CY, Tan KSW (2019) Successful genetic transfection of the colonic protistan parasite *Blastocystis* for reliable expression of ectopic genes. *Sci Rep* **9**:3159 https://doi.org/10.1038/s41598-019-39094-5 | PubMed

Lightner DA, Holmes DL, McDonagh AF (1996) On the acid dissociation constants of bilirubin and biliverdin: pKa values from 13C NMR spectroscopy. *Journal of Biological Chemistry* **271**:2397-2405 https://doi.org/10.1074/jbc.271.5.2397 | PubMed

Maiti A, Buffalo CZ, Saurabh S, Montecinos-Franjola F, Hachey JS, Conlon WJ, Tran GN, Hassan B, Walters KJ, Drobizhev M, *et al.* (2023) Structural and photophysical characterization of the small ultra-red fluorescent protein. *Nat Commun* **14**:4155 https://doi.org/10.1038/s41467-023-39776-9 | PubMed

Mirza H, Teo JDW, Upcroft J, Tan KSW (2011) A rapid, high-throughput viability assay for *Blastocystis* spp. reveals metronidazole resistance and extensive subtype-dependent variations in drug susceptibilities. *Antimicrob Agents Chemother* **55**:637-648 https://doi.org/10.1128/AAC.00900-10 | PubMed

Nagel R, Gray C, Bielefeldt-Ohmann H, Traub RJ (2015) Features of *Blastocystis* spp. in xenic culture revealed by deconvolutional microscopy. *Parasitol Res* **114**:3237-3245 https://doi.org/10.1007/s00436-015-4540-x | PubMed

Ostrow JD, Celic L (1984) Bilirubin chemistry, ionization and solubilization by bile salts. *Hepatology* **4**:38S-45S https://doi.org/10.1002/hep.1840040807 | PubMed

Piperni E, Nguyen LH, Manghi P, Kim H, Pasolli E, Andreu-Sánchez S, Arrè A, Bermingham KM, Blanco-Míguez A, Manara S, *et al.* (2024) Intestinal *Blastocystis* is linked to healthier diets and more favorable cardiometabolic outcomes in 56,989 individuals from 32 countries. *Cell* **187**:4554-4570.e18. https://doi.org/10.1016/j.cell.2024.06.018 | PubMed

Porzberg N, Gries K, Johnsson K (2025) Exploiting covalent chemical labeling with self-labeling proteins. *Annual Review of Biochemistry* **94**:29-58 https://doi.org/10.1146/annurev-biochem-030222-121016 | PubMed

Pronobis MI, Deuitch N, Peifer M (2016) The miraprep: A protocol that uses a miniprep kit and provides maxiprep yields. *PLOS One* **11**:e0160509 https://doi.org/10.1371/journal.pone.0160509 | PubMed

Pyrihová E, King MS, King AC, Toleco MR, van der Giezen M, Kunji ER (2024) A mitochondrial carrier transports glycolytic intermediates to link cytosolic and mitochondrial glycolysis in the human gut parasite *Blastocystis*. *eLife* **13**:RP94187 https://doi.org/10.7554/eLife.94187 | PubMed

Remcho TP, Guggilapu SD, Cruz P, Nardone GA, Heffernan G, O'Connor RD, Bewley CA, Wellems TE, Lane KD. (2020) Regioisomerization of antimalarial drug WR99210 explains the inactivity of a commercial stock. *Antimicrob Agents Chemother* **65**:e01385-20 https://doi.org/10.1128/AAC.01385-20 | PubMed

Rodriguez EA, Tran GN, Gross LA, Crisp JL, Shu X, Lin JY, Tsien RY (2016) A far-red fluorescent protein evolved from a cyanobacterial phycobiliprotein. *Nat Methods* **13**:763-769 https://doi.org/10.1038/nmeth.3935 | PubMed

Saimi D, Chen Z (2023) Chemical tags and beyond: Live-cell protein labeling technologies for modern optical imaging. *Smart Mol* **1**:e20230002 https://doi.org/10.1002/smo.20230002 | PubMed

Scanlan PD, Stensvold CR (2013) *Blastocystis*: getting to grips with our guileful guest. *Trends in Parasitology* **29**:523-529 https://doi.org/10.1016/j.pt.2013.08.006 | PubMed

Šejnohová A, Koutenská M, Jirků M, Brožová K, Pavlíčková Z, Kadlecová O, Cinek O, Maloney JG, Santín M, Petrželková KJ, *et al.* (2024) A cross-sectional survey of *Blastocystis* sp. and *Dientamoeba fragilis* in non-human primates and their caregivers in Czech zoos. *One Health* **19**:100862 https://doi.org/10.1016/j.onehlt.2024.100862 | PubMed

Stechmann A, Hamblin K, Pérez-Brocal V, Gaston D, Richmond GS, van der Giezen M, Clark CG, Roger AJ. (2008) Organelles in *Blastocystis* that blur the distinction between mitochondria and hydrogenosomes. *Current Biology* **18**:580-585 https://doi.org/10.1016/j.cub.2008.03.037 | PubMed

Stensvold CR, van der Giezen M. (2018) Associations between gut microbiota and common luminal intestinal parasites. *Trends in Parasitology* **34**:369-377 https://doi.org/10.1016/j.pt.2018.02.004 | PubMed

Tan SW, Singh M, Thong KT, Ho LC, Moe KT, Chen XQ, Ng GC, Yap EH (1996a) Clonal growth of *Blastocystis hominis* in soft agar with sodium thioglycollate. *Parasitol Res* **82**:737-739 https://doi.org/10.1007/s004360050194 | PubMed

Tan SW, Singh M, Yap EH, Ho LC, Moe KT, Howe J, Ng GC (1996b) Colony formation of *Blastocystis hominis* in soft agar. *Parasitol Res* **82**:375-377 https://doi.org/10.1007/s004360050130 | PubMed

Tan KSW, Ng GC, Quek E, Howe J, Ramachandran NP, Yap EH, Singh M (2000) *Blastocystis hominis*: A simplified, high-efficiency method for clonal growth on solid agar. *Exp. Parasitol* **96**:9-15 https://doi.org/10.1006/expr.2000.4544 | PubMed

Tan KSW (2008) New insights on classification, identification, and clinical relevance of *Blastocystis* spp. *Clin Microbiol Rev* **21**:639-665 https://doi.org/10.1128/CMR.00022-08 | PubMed

Toleco MR, van der Giezen M. (2025) A simple and universal quasi-modular cloning system using NEBuilder® HiFi DNA assembly kit. *BioTechniques* **77**:257-262 https://doi.org/10.1080/07366205.2025.2542012 | PubMed

Tsaousis AD, Hamblin KA, Elliott CR, Young L, Rosell-Hidalgo A, Gourlay CW, Moore AL, van der Giezen M. (2018) The human gut colonizer *Blastocystis* respires using complex II and alternative oxidase to buffer transient oxygen fluctuations in the gut. *Front Cell Infect Microbiol* **8**:371 https://doi.org/10.3389/fcimb.2018.00371 | PubMed

Vara JA, Pulido D, Lacalle RA, Jiménez A (1988) Two genes in *Streptomyces alboniger* puromycin biosynthesis pathway are closely linked. *Gene* **69**:135-140 https://doi.org/10.1016/0378-1119(88)90386-1 | PubMed

Wu Z, Mirza H, Tan KSW (2014) Intra-subtype variation in enteroadhesion accounts for differences in epithelial barrier disruption and is associated with metronidazole resistance in *Blastocystis* subtype-7. *PLoS Negl Trop Dis* **8**:e2885 https://doi.org/10.1371/journal.pntd.0002885 | PubMed

Yason JA, Liang YR, Png CW, Zhang Y, Tan KSW (2019) Interactions between a pathogenic *Blastocystis* subtype and gut microbiota: *in vitro* and *in vivo* studies. *Microbiome* **7**:30 https://doi.org/10.1186/s40168-019-0644-3 | PubMed

Yason JA, Tan KSW (2018) Membrane surface features of *Blastocystis* subtypes. *Genes* **9**:417 https://doi.org/10.3390/genes9080417 | PubMed

Yoshikawa H, Hayakawa A (1996) Freeze-fracture cytochemistry of membrane cholesterol in *Blastocystis hominis*. *International Journal for Parasitology* **26**:1111-1114 https://doi.org/10.1016/S0020-7519(96)80010-5

Záhonová K, Low RS, Warren CJ, Cantoni D, Herman EK, Yiangou L, Ribeiro CA, Phanprasert Y, Brown IR, Rueckert S, *et al.* (2023) Evolutionary analysis of cellular reduction and anaerobicity in the hyper-prevalent gut microbe *Blastocystis*. *Current Biology* **33** https://doi.org/10.1016/j.cub.2023.05.025 | PubMed

Zheng X, Gallot G (2020) Dynamics of cell membrane permeabilization by saponins using terahertz attenuated total reflection. *Biophys J* **119**:749-755 https://doi.org/10.1016/j.bpj.2020.05.040 | PubMed

Zhu X, Ricci-Tam C, Hager ER, Sgro AE (2023) Self-cleaving peptides for expression of multiple genes in *Dictyostelium discoideum*. *PLOS One* **18**:e0281211 https://doi.org/10.1371/journal.pone.0281211 | PubMed

Zucker SD, Goessling W, Hoppin AG (1999) Unconjugated bilirubin exhibits spontaneous diffusion through model lipid bilayers and native hepatocyte membranes. *J Biol Chem* **274**:10852-10862 https://doi.org/10.1074/jbc.274.16.10852 | PubMed

Armengaud J, Pible O, Gaillard JC, Cian A, Gantois N, Tan KSW, Chabé M, Viscogliosi E (2017) Proteogenomic of Blastocystis sp. subtype 4 isolate WR1. ProteomeXchange. ID PXD006588 https://proteomecentral.proteomexchange.org/?pxid=PXD006588

Peer reviews

Reviewer #1 (Public review):

Summary:

This paper presents a toolkit for the transformation of Blastocystis. The authors have screened a number of selectable agents, promoters and reporter genes and present their findings. This resource will be of immense use to those in the Blastocystsis field, as well as those seeking to establish transformation tools in other species where such tools do not yet exist. Establishing new transformation tools is extremely challenging, and the authors have done an excellent job.

Strengths:

The authors have carried out a systematic screen of promoters, reporter genes and selectable agents. They have screened numerous for each, and all the data is presented. It is good to see when things did not work as well as when things did, so this data set is extremely useful indeed.

Weaknesses:

The findings are reported by reporter gene assay (microscopy). No evidence is given using genetics. The authors claim that the DNA is maintained episomally. However, could it be possible that there is integration? No PCRS/RT-PCRs are shown (although it can safely be assumed that the DNA/RNA is present where the transformation was successful), nor are any Western blots. These would have been useful to show that the P2A ribosomal skipping had occurred, and that proteins were expressed individually rather than as a polyprotein.

https://doi.org/10.7554/eLife.111816.1.sa2

Reviewer #2 (Public review):

This manuscript presents a substantial technical advance for the genetic manipulation of Blastocystis by establishing an integrated workflow for stable episomal transgenesis, antibiotic selection, clonal recovery, and reporter-based imaging in the ST7-B subtype. The study is particularly valuable because it combines multiple previously fragmented approaches into a coherent and practically applicable toolkit, including endogenous regulatory elements, optimized electroporation conditions, selectable markers, and anaerobic compatible fluorescent reporters. This methodological work greatly expands the molecular toolbox and future studies focused on both basic and infection biology can now build on the ability to express and localize proteins in fixed as well as live cells.

The microscopy data are convincing and clearly demonstrate functional reporter expression and successful recovery of stable transgenic lines. Nevertheless, because this is primarily a methodological paper, the study would be further strengthened by the inclusion of Western blot validation of reporter expression and bicistronic constructs. In particular, biochemical analysis of the P2A-containing constructs would help assess the efficiency of ribosomal skipping and exclude the possible presence of uncleaved fusion proteins, thereby providing

stronger support for the interpretation of the imaging data and the functionality of the expression system.

https://doi.org/10.7554/eLife.111816.1.sa1

Reviewer #3 (Public review):

Summary:

The primary objective of this study was to establish a practical and functional framework for the propagation of stable transgenic cell lines of Blastocystis, a common animal gut microeukaryote. Although the work focused on Blastocystis ST7-B, a subtype with relatively low prevalence in humans, this choice is justified by its association with more frequent negative health effects. Beyond their relevance to the medical field, the methodological advances described here have the potential to also expand cell biology studies of this anaerobic organism, including its unusual mitochondria and redox metabolism.

Strengths:

Prior to this work, genetic tools for Blastocystis were very limited, relying on a single strong promoter-terminator combination. The authors successfully expanded the available promoter set across a range of expression strengths by testing two dozen variants in luciferase-based assays. Critically, they developed an integrated workflow from a modular transgenic construct design, to an expanded inventory of molecular components (promoters, reporters), optimized DNA delivery, stepwise antibiotic resistance-mediated clonal selection and propagation, and to reporter validation. The evaluation of several anaerobiosis-compatible labeling strategies for live (and fixed) cell optical imaging will be particularly useful, with the SNAP-tag system appearing especially promising for Blastocystis.

Weaknesses:

The presented data generally provide solid support for the conclusions that the work reached, but clarification of reasoning and several inconsistencies, as well as amendments to the visual presentation of the data, would be highly beneficial, as detailed below.

(1) Episomal persistence of the construct:

The manuscript repeatedly assumes, including in its title, that constructs persist in Blastocystis in their episomal form, but no direct evidence is provided. Although this interpretation is plausible, it should be identified more clearly as provisional. Nuclear genomic integration (e.g., via NHEJ) remains a possible explanation unless supporting evidence or rationale is provided to exclude it. Testing whether the phenotype persists without drug-mediated selection in the generated transgenic cell lines would help strengthen the case for episomal maintenance.

(2) Promoters and terminators:

2.1) There is a discrepancy between the claimed number of loci (14), from which promoters used to drive luciferase expression were derived, and those detailed as having been actually generated in Table 1 (11). This inconsistency should be corrected or explained, as it creates uncertainty around the accuracy of the dataset.

2.2) Based on the presented evidence, constructs benchmarked in bioluminescence assays differed only in their promoter composition. Although terminator selection is mentioned in the Methods section, no additional details are provided; for instance, Table 1 and Figure 2 only list 23 promoters in total. Figure 2A likewise shows only promoter-dependent variation. If the terminator was held constant (LeguP1?), this should be stated explicitly. The authors

may then consider revising the wording of having tested "23 promoter-terminator pairs" to better reflect that only promoters varied.

2.3) Promoter benchmarking was done with a plasmid lacking a selection marker, so it is unclear how the maintenance of the luciferase construct was ensured. Without selection, the observed reporter intensity could reflect differential or stochastic plasmid retention rather than promoter strength alone. The luminescence assay was performed 16-18 hours after transfection, but the rationale for this particular timeframe should be explained. In this context, the authors should explicitly state whether the experiments shown in Fig.2A represent biological triplicates or technical triplicates from a single transfection.

(3) Figure 2:

3.1) Several aspects of the current design may lead to ambiguity for the reader. The boxplots are colour-coded, but it is unclear whether the colours carry meaning or are purely decorative. Because the data are already spatially separated into bins, additional random colouring is redundant and may suggest distinctions that are not intended. In addition, part A of Figure 2 is split into two panels, with the scale for the left panel shown in the right panel and some of the boxplot colours falling in the range of the scale, but not in line with their counterparts in the left panel. Because the colour use is not consistent, it is difficult to tell whether the same scale should be applied to both panels or how it should be interpreted.

3.2) The left panel of part A uses a diverging blue-white-red colour scheme, which is most appropriate when the midpoint represents a meaningful central value such as zero. Because the values shown in this graph are only positive, a non-diverging 2-colour scale or a colour palette such as 'viridis' would make the plot easier to interpret.

3.3) A black background should be avoided: 'B' and 'C' labels are invisible, and it draws attention to a distracting design feature rather than the data themselves.

(4) Figure 3:

4.1) Individual snapshots should be separated more clearly, either by using a white background or by adding visible borders to make the overall composition clearer. As currently displayed, some boundaries between fluorescent channels resemble image artifacts rather than intentional panel divisions.

4.2) In parts B-D, the legend should explain more clearly what each image shows, and the figure itself would benefit from annotations. There seem to be three sub-panels in each 'condition' of part B (as well as C and D): while the middle and rightmost panel can be easily inferred to represent the fluorescent protein and bright-field image, what the leftmost panels represent is not specified. If DAPI was used to dye DNA, an explanation why mostly multiple labelled regions are visible should be provided.

4.3) Cell morphology and appearance differ markedly between UnaG/smURFP and SNAP-tag images, which should be explained. A microscope issue is mentioned in the main text, but if that was the cause, the authors should consider replacing the images, as the current distortions complicate interpretation.

https://doi.org/10.7554/eLife.111816.1.sa0